⌘ *Author's Choice*

THE JOURNAL OF BIOLOGICAL CHEMISTRY VOL. 286, NO. 7, pp. 5691–5707, February 18, 2011

PC4/Tis7/IFRD1 Stimulates Skeletal Muscle Regeneration and Is Involved in Myoblast Differentiation as a Regulator of MyoD and NF-κB*[S]

Received for publication, July 13, 2010, and in revised form, November 4, 2010 Published, JBC Papers in Press, December 2, 2010, DOI 10.1074/jbc.M110.162842

Laura Micheli[‡1,2], Luca Leonardi[‡2], Filippo Conti[‡2], Giovanna Maresca[‡], Sandra Colazingari[‡], Elisabetta Mattei[‡], Sergio A. Lira[§], Stefano Farioli-Vecchioli[‡], Maurizia Caruso[‡], and Felice Tirone[‡3]

From the [‡]Istituto di Neurobiologia e Medicina Molecolare, Consiglio Nazionale delle Ricerche, Fondazione S. Lucia, Via del Fosso di Fiorano 64, 00143 Rome, Italy and the [§]Immunology Institute, Mount Sinai School of Medicine, New York, New York 10029

In skeletal muscle cells, the PC4 (Tis7/Ifrd1) protein is known to function as a coactivator of MyoD by promoting the transcriptional activity of myocyte enhancer factor 2C (MEF2C). In this study, we show that up-regulation of *PC4 in vivo* in adult muscle significantly potentiates injury-induced regeneration by enhancing myogenesis. Conversely, we observe that *PC4* silencing in myoblasts causes delayed exit from the cell cycle, accompanied by delayed differentiation, and we show that such an effect is *MyoD*-dependent. We provide evidence revealing a novel mechanism underlying the promyogenic actions of PC4, by which PC4 functions as a negative regulator of NF-κB, known to inhibit *MyoD* expression post-transcriptionally. In fact, up-regulation of *PC4* in primary myoblasts induces the deacetylation, and hence the inactivation and nuclear export of NF-κB p65, in concomitance with induction of *MyoD* expression. On the contrary, *PC4* silencing in myoblasts induces the acetylation and nuclear import of p65, in parallel with a decrease of MyoD levels. We also observe that PC4 potentiates the inhibition of NF-κB transcriptional activity mediated by histone deacetylases and that PC4 is able to form trimolecular complexes with p65 and HDAC3. This suggests that PC4 stimulates deacetylation of p65 by favoring the recruitment of HDAC3 to p65. As a whole, these results indicate that PC4 plays a role in muscle differentiation by controlling the *MyoD* pathway through multiple mechanisms, and as such, it positively regulates regenerative myogenesis.

Skeletal myoblast differentiation is a multistep process characterized by permanent exit from the cell cycle, maturation into mononucleated myocytes, and fusion in multinucleated myotubes. This differentiation program is controlled by the basic helix-loop-helix family of myogenic regulatory factors (MRFs),[4] including *MyoD*, *Myf-5*, *myogenin*, and *MRF4/Myf6/Herculin* (Refs. 1–6 and reviewed in Ref. 7). The MRFs form heterodimers with the ubiquitously expressed basic helix-loop-helix E proteins to bind to a consensus sequence, termed E-box, present in the regulatory regions of many muscle-specific genes (8). Activation of muscle gene expression by MRFs is also dependent on their functional interaction with members of the myocyte enhancer factor 2 (*MEF2*) family of transcription factors, which bind to a conserved A/T-rich sequence often located in close proximity to E-boxes in muscle gene control regions (9, 10).

The gene *PC4*, also known as *Tis7* or *IFRD1* (in rat, mouse, and human, respectively), participates to the process of skeletal muscle cell differentiation. In fact, inhibition of *PC4* function in C2C12 myoblasts, by antisense *PC4* cDNA transfection or microinjection of anti-PC4 antibodies, prevents their morphological and biochemical differentiation (11). Recently, a role for *PC4* in muscle differentiation has been observed also *in vivo*. Muscles from mice lacking *Tis7* display decreased protein and mRNA levels of MyoD, myogenin, and laminin-alfa2 (12). Remarkably, it was observed that myofibers of *Tis7* null 24-month-old mice were reduced in diameter and number and that after muscle crash damage in young mice there was a delay in regeneration, as defined by an alteration of the isometric contractile properties of skeletal muscle. The misregulation of key regulatory proteins and the reduced regeneration occurring in adult muscles of *Tis7* null mice suggest that Tis7 plays an important role in the differentiation of adult muscle stem cells. However, no indication about the underlying molecular mechanism(s) was obtained from the knock-out experiments.

In this regard, we have recently found that *PC4* (as we refer to both the mouse and rat gene) cooperates with MyoD at inducing the transcriptional activity of MEF2C by counteracting the inhibition exerted by histone deacetylase 4 (HDAC4) on MEF2C. This relies on the ability of PC4 to bind selectively MEF2C, thus inhibiting its interaction with HDAC4 (13). Therefore, PC4 appears to act as a positive cofactor of MyoD

* This work was supported in part by Telethon Grant GGP00582, Fondo Investimenti Ricerca di Base Project RBIN04P4ET, and Progetti di Ricerca Interesse Nazionale Project 20074Z3H3N_003.

[S] The on-line version of this article (available at http://www.jbc.org) contains supplemental Figs. S1–S3.

⌘ *Author's Choice*—Final version full access.

[1] Supported by Finanziaria Laziale di Sviluppo Regione Lazio.

[2] These authors contributed equally to this work.

[3] To whom correspondence should be addressed. Tel.: 39-06-501703184; Fax: 39-06-501703313; E-mail: tirone@inmm.cnr.it.

[4] The abbreviations used are: MRF, myogenic regulatory factor; GM, growth medium; DM, differentiation medium; nt, nucleotide; rtTA, reverse tetracycline-regulated TransActivator; CT, control; TG, transgene; P, postnatal day; TA, tibialis anterior; TRITC, tetramethylrhodamine isothiocyanate; TRE, tetracycline-responsive element; HDAC, histone deacetylase; MCK, muscle creatine kinase.

(13). *MyoD* knock-out mice models indicate a unique requirement of *MyoD* during adult muscle regeneration, rather than during embryonic muscle development, where other myogenic regulatory factors can compensate (14). Remarkably, *PC4* is expressed *in vivo* in adult skeletal muscle, although it is barely detectable during embryonic development (15), which suggests a prevalent role for *PC4* in *MyoD*-dependent post-developmental myogenesis.

However, an important question still unanswered is whether *PC4* plays an active part *in vivo* as inducer of adult muscle regeneration. A second question is whether the ability of PC4 to coactivate MyoD is at the origin of the role played by *PC4* in myoblast differentiation or if other mechanisms are involved. To answer these questions, we analyzed the muscle regeneration potential of a mouse model where *PC4* was up-regulated in skeletal muscle, as well as the differentiation process of myoblasts deprived of PC4 expression through RNA interference. We observed that up-regulation of *PC4 in vivo* potentiated injury-induced muscle regeneration and that deprivation of PC4 in myoblasts led to down-regulation of *MyoD* expression, which was responsible for delayed exit from the cell cycle and impairment of terminal differentiation. Furthermore, our data reveal a novel mechanism underlying the promyogenic activity of PC4; in fact, we found that PC4 acts as a repressor of NF-κB transcriptional activity, which is known to inhibit *MyoD* mRNA accumulation. We also found that PC4 represses the activity of NF-κB by enhancing the HDAC-mediated deacetylation of the p65 subunit. Our results indicate that *PC4* can influence muscle regeneration acting as a pivotal regulator of the *MyoD* pathway through multiple mechanisms.

EXPERIMENTAL PROCEDURES

Transgene Constructs—The TRE-*PC4* construct (pUHD10-3-*PC4*) was generated by subcloning the *PC4* (rat sequence) open reading frame (ORF; 1.38 kb (16)) into the EcoRI site of pUHD10-3 (17). The 2.3-kb transgene (PacI-HindIII fragment of pUHD10-3-*PC4*, where the PacI site was added in close proximity to the XhoI site of pUHD10-3) included the *PC4* ORF under the control of seven copies of the tetracycline-responsive element (TRE), followed by the minimal cytomegalovirus (CMV) promoter (PacI-BamHI fragment) and the simian virus 40 (SV40) poly(A) site downstream of the *PC4* ORF (BamHI-HindIII fragment).

The activator transgene, CMV-*βactin*-rtTA, which produces the reverse tetracycline-regulated transactivator (rtTA) that binds and activates TRE-*PC4* in the presence of tetracycline (or of its analog doxycycline), was constructed as described previously, by cloning the rtTA sequence between the CMV enhancer/chicken β-actin promoter and the rabbit β-globin polyadenylation signal (18).

Transgenic Animals and Genotyping—The bitransgenic CMV-*βactin*-rtTA/TRE-*PC4* mouse line is the progeny of two mouse lines, each carrying a transgene as follows: the CMV-*βactin*-rtTA transgene, encoding rtTA driven by the β-actin promoter, and the TRE-*PC4* transgene, carrying the *PC4* coding region under control of TRE (see above). The bitransgenic CMV-*βactin*-rtTA/TRE-*PC4* mouse line used for experiments was isogenic, having been previously interbred for at least six generations. The TRE-*PC4* transgenic line was generated by injecting into zygotes derived from 4- to 8-week-old FVB female mice the purified 2.3-kb PacI-HindIII DNA fragment of TRE-*PC4* (5 ng/ml; see above). Injected embryos were transferred to the oviducts of pseudopregnant FVB foster females aged 2–8 months, as described previously (19). The identification of transgenic founders was conducted by PCR analysis on genomic DNA from tail tips using primers that amplified the whole transgene, being complementary to regions of the vector pUHD10-3-*PC4* upstream and downstream to the *PC4* insert (forward, 5′-CCACTCCCTATCAGTGATAG3–3′; backward, 5′-CTCATCAATGTATCTTATCATGTC-3′). Further controls were also performed by using other sets of primers internal and external to the *PC4* insert. Screening of transgenic mice for routine genotyping was performed by PCR, using the forward primer complementary to a region of the vector immediately upstream to the *PC4* insert (5′-TGACCTCCATAGAAGACACC-3′) and the backward primer within the *PC4* transgene (5′-AATCCCGTTCCTCCACAG-3′). The production and characterization of mice carrying the rtTA transgene under the control of CMV enhancer/chicken β-actin promoter have been described previously (18). Primers used to identify CMV-*βactin*-rtTA transgenic animals amplified 945 bp of the tTA transgene as follows: ftTA2 (5′-TGCTTAATGAGGTCGGAATCG-3′) and rtTA2 (5′-CCAAGGGCATCGGTAAACATC-3′).

Cardiotoxin, Histology, and Quantification of Myofibers and Satellite Cells—To evaluate the muscle regeneration process, we used bitransgenic CMV-*βactin*-rtTA/TRE-*PC4* and control mice (the progeny of bitransgenic mice that did not inherit the TRE-*PC4* transgene), and both were treated with doxycycline (2 μg/ml in drinking water) to equalize any possible effect of doxycyline on regeneration. Injury was performed on the tibialis anterior (TA) muscle of 2-month-old mice by injecting 20 μl of 10 μM cardiotoxin. Regeneration was evaluated in mice with the transgene activated by doxycycline at P30 and analyzed at P60. Mice were killed 5, 7, and 20 days after cardiotoxin injection in TA; then TA muscles were collected and embedded in OCT (Tissue-Tek; Sakura Finetek Europe, The Netherlands), and 10-μm cryosections were cut and processed for histological analysis through immunohistochemistry. At least three animals from each group (control and bitransgenic mice) per time point were analyzed. Images using a 20× lens objective were captured in three sections per group in the regenerative area, and the number of central nucleated myofibers was counted. Results are reported as the average number of fibers per area. In addition, the area of the central nucleated fibers was measured. A minimum of 2000 muscle fibers per group per time point was analyzed. Satellite cells were quantified by counting Pax7-positive cells and the total fibers in sections in the belly of the TA. Five animals for each group were analyzed. Mice were treated with doxycyline from gestation until they were killed at P45.

Isolation and Culture of Primary Myoblasts—Primary myoblasts were isolated as described by Rando and Blau (20). Briefly, adult hindlimb muscles from 2-month-old mice were minced into a coarse slurry using razor blades and enzymati-

cally digested at 37 °C in PBS 1×, 2 mg/ml collagenase/dispase (Roche Diagnostics). The slurry was passed through a 40-μm cell strainer (BD Biosciences). The filtrate was centrifuged at 350 × *g* to sediment the dissociated cells; the pellet was resuspended in growth medium, and the suspension was preplated for 2 h on noncoated dishes. The medium containing floating cells was then centrifuged, and cells were plated on collagen-coated dishes.

Primary myoblasts were grown in Ham's F-10 nutrient mixture (Invitrogen), containing penicillin (200 units/ml) and streptomycin (200 μg/ml), and supplemented with 20% fetal bovine serum (HyClone, Logan, UT) and 5 ng/ml basic FGF (PeproTech Inc., Rocky Hill, NJ). Cells were differentiated in DMEM with 5% horse serum. Tissue culture dishes were coated with 0.01% type I collagen (Sigma). Cells were grown in a humidified incubator at 37 °C in 5% CO_2.

Cell Lines—C2C12 cells from the 16th passage were obtained from H. Blau (Stanford University, Stanford, CA) and propagated in GM (Dulbecco's modified medium (DMEM) with 20% fetal bovine serum) in a humidified atmosphere of 10% CO_2 at 37 °C. Differentiation was obtained by shifting the cultures to DM (DMEM with 2% horse serum), with a change of medium every 24 h. C3H10T1/2 fibroblasts were also grown in GM or DM.

Design of siRNAs—The 19-nucleotide siRNA sequences specific to *PC4/Tis7* (*i.e.* both mouse and rat sequences) were designed by the on-line Design Tool software (MWG, Ebersberg, Germany). Candidate sequences were used to synthesize a pair of 64-mer oligonucleotides that were annealed and cloned in the pSUPER.retro.puro siRNA expression vector, according to the manufacturer's instructions (Oligoengine, Inc., Seattle) (21). The *PC4/Tis7* siRNA sequences were as follows: *PC4*/2, 5′-GAGAGCAGATGTTGGAGAA-3′; *PC4*/7, 5′-GCGCATGTATATTGATAGC-3′. The control sequence from the luciferase gene was 5′-ACGGATTACCAGGGATTTC-3′. The presence of the correct sequence cloned in pSUPER.retro.puro was confirmed by sequencing.

Generation of Recombinant Viruses and Infections—The pSUPER.retro.puro-*PC4*/2, pSUPER.retro.puro-*PC4*/7, pSUPER.retro.puro-LUC constructs, or the empty pSUPER.retro.puro vector (Oligoengine, Inc.) were transfected into the packaging Phoenix helper cells using Lipofectamine 2000 (Invitrogen). The supernatants were collected after 48 and 72 h and used for infection. C2C12 myoblasts or C3H10T1/2 cells were plated in 90-mm dishes (6×10^5 cells) and infected the first time with the viral supernatant after 24 h and then a second time after 48 h. 72 h after plating, the cells were split and selected with puromycin (2 μg/ml) in GM for 4 days. Infected cells were then reseeded to analyze protein and mRNA expression (60-mm dishes; 4×10^5 cells) and cell cycle progression (60-mm dishes; 2×10^5 cells) or for immunofluorescence staining with myosin heavy chain (MHC) (35-mm dishes; 2×10^5 cells) or for transient luciferase reporter transfection experiments (35-mm dishes; $5–7 \times 10^5$ cells).

Plasmids, Expression Vectors, and Retroviruses—pcDNA3-FLAG-*MyoD* was a gift of V. Sartorelli. pCDNA1-*MEF2C*, 4RE-luciferase, and 3×MEF2-luciferase were provided by E. Olson (22, 23). pSCT-*PC4* and HA-*MEF2C* had been previously generated by us (11, 13). pBABE-puro-*MyoD* was obtained from P. Amati, and the generation of pBABE-*MyoD* retroviruses was performed as described previously (24). pcDNA3.1-*Myc-HDAC4* was provided by T. Kouzarides and pcDNA3.1-*Myc-HDAC3* by M. A. Lazar (25).

Immunocytochemistry and Confocal Microscopy—MHC was detected by immunofluorescence staining in C2C12 cell cultures grown on 35-mm dishes and fixed for 10 min at room temperature in phosphate-buffered saline (PBS) containing 3.75% paraformaldehyde. Cells were then washed in PBS, permeabilized by a 5-min incubation in 0.2% Triton X-100 in PBS, washed in PBS, and incubated for 60 min at room temperature with the mouse monoclonal anti-MHC (Developmental Studies Hybridoma Bank, University of Iowa; clone MF20; 1:1). The antigen was revealed by fluorescein isothiocyanate (FITC)-conjugated (Jackson ImmunoResearch, West Grove, PA) secondary antibody. Immunofluorescence was observed by using an Olympus BX51 microscope (Tokyo, Japan) with a Diagnostic Instruments digital camera (model 1.3.0).

Normal and lesioned TA skeletal muscles were dissected from adult mice (2.5 months), embedded in Tissue-Tek OCT (Sakura, Torrance, CA), and frozen in liquid N_2-cooled isopentane. Immunocytochemistry of muscle was performed on serial sections cut transversely at a 9-μm thickness at −25 °C in a cryostat. Cryosections were fixed in 4% formaldehyde, quenched with 100 mM glycine, permeabilized with 0.3% Triton X-100, and blocked in PBS containing 3% normal donkey serum and 0.3% Triton X-100. Sections were then incubated overnight with an antibody against laminin (Sigma; rabbit polyclonal L9393; 1:400) diluted in blocking solution. As for Pax7 immunodetection, TA cryosections fixed in 4% paraformaldehyde were permeabilized in methanol and treated with hot 0.01 M citric acid for 10 min for antigen retrieval. Dividing muscle progenitor cells were detected by visualizing the incorporation of bromodeoxyuridine (BrdU), injected daily (95 mg/kg intraperitoneal) during 4 days before killing mice for analysis (at P10, P15, and P30). BrdU incorporation was detected following pretreatment of sections to denature the DNA, with 2 N HCl for 45 min at 37 °C and then with 0.1 M sodium borate buffer, pH 8.5, for 10 min. Afterward, sections were incubated with a rat monoclonal antibody against BrdU (Serotec, Raleigh, NC; MCA2060; 1:150).

Antigens were revealed by Cy2-conjugated donkey anti-rabbit, TRITC-conjugated donkey anti-mouse or donkey anti-rat secondary antibodies (all from Jackson ImmunoResearch). Nuclei were counterstained by Hoechst 33258. Images of the immunostained sections were obtained by laser scanning confocal microscopy using a TCS SP5 microscope (Leica Microsystems, Wetzlar, Germany). All analyses were performed in sequential scanning mode to rule out cross-bleeding between channels.

Differentiation and Fusion Index—Differentiation index and fusion index were calculated as described previously (26, 27). Differentiation index corresponded to the percent ratio of cells labeled by MHC to the total number of cells, as detected by the staining of nuclei with Hoechst 33258 dye. The fusion

index was measured as percent ratio of the number of nuclei detected in MHC-labeled cells to the total number of nuclei.

Immunoblots and Antibodies—C2C12 myoblasts and C3H10T1/2 fibroblasts, either control-infected or shRNA *PC4*-infected, or primary myoblasts from Tg *PC4* were lysed by sonication in buffer containing 50 mM Tris-HCl, pH 7.4, 150 mM NaCl, 1 mM EDTA, 0.2% Nonidet P-40, with protease inhibitors 1 mM Na_3VO_4, 10 mM 2-glycerophosphate, 10 mM NaF, 5 mM ATP, 5 mM $MgCl_2$. In experiments analyzing the protein acetylation state, deacetylase inhibitors were added (5 mM sodium butyrate and 600 nM trichostatin A). Transgenic mouse tissues were homogenized in Laemmli buffer (170 mM Tris-HCl, pH 6.8, 9% glycerol, 2.1% SDS, 4% 2-mercaptoethanol, with protease inhibitors). Proteins were electrophoretically separated by SDS-PAGE and transferred to nitrocellulose filters, as described previously (28). Immunoblots were performed hybridizing filters to the following mouse monoclonal antibodies: against PC4/Tis7 (Sigma; T2576; 1:400); myogenin (Developmental Studies Hybridoma Bank; clone IF5D7/2; 1:3); MyoD (DakoCytomation, Glostrup, Denmark; M3512; 1:500); Pax7 (Developmental Studies Hybridoma Bank; 1:1); myosin heavy chain (Developmental Studies Hybridoma Bank; clone MF20; 1:3); sarcomeric α-actin (Sigma; A2172; 1:2000); cyclin D1 (Santa Cruz Biotechnology, Santa Cruz, CA; clone 72-13G, sc450; 1:200); pRb (BD Biosciences; clone G3-245, 554136; 1:1000); α-tubulin (Sigma; clone 5C5, A2172; 1:2000); FLAG (Sigma; clone M2, F3165; 1:1000); c-*myc* tag (Santa Cruz Biotechnology; clone 9E10; 1:100); or to the following rabbit polyclonal antibodies against: MEF2C (Cell Signaling Technology Inc., Danvers, MA; 9792; 1:500); MEF2 (Santa Cruz Biotechnology; sc313; 1:200); Myf5 (Santa Cruz Biotechnology; sc302; 1:200); cyclin D3 (Santa Cruz Biotechnology; sc182; 1:200); cyclin A (Santa Cruz Biotechnology; sc596; 1:400); cyclin E (Santa Cruz Biotechnology; sc481; 1:200); p21 (Santa Cruz Biotechnology; sc397; 1:200); p65 (Santa Cruz Biotechnology; sc372; 1:1000); p65 acetyl-K310 (Abcam, Cambridge, UK; ab52175; 1:500); or goat polyclonal antibody against HDAC4 (Santa Cruz Biotechnology; sc5246; 1:200).

Immunoprecipitation—C2C12 myoblasts clone S4 grown in 90-mm dishes, transfected with *Myc-HDAC3* or pcDNA3, were lysed by sonication in buffer containing 50 mM Tris-HCl, pH 7.4, 150 mM NaCl, 1 mM EDTA, 0.2% Nonidet P-40, protease inhibitors, 1 mM Na_3VO_4, 10 mM 2-glycerophosphate, 10 mM NaF, 5 mM ATP, 5 mM $MgCl_2$, 5 mM sodium butyrate, 600 nM trichostatin A. Then 0.3 mg of total protein lysate was immunoprecipitated overnight with agarose-conjugated rabbit polyclonal anti-p65 (Santa Cruz Biotechnology; sc372AC), or with agarose-conjugated control IgG (Santa Cruz Biotechnology; normal rabbit IgG; sc2345).

RNA Extraction, Real Time RT-PCR—Total cellular RNA, obtained from tissues or cells according to the procedure of Chomczynski and Sacchi (29), was reverse-transcribed as described previously (28). Total RNA was analyzed by real time RT-PCR amplification, using TaqMan probe-based fluorogenic 5′-nuclease chemistry in duplicate samples and a 7900HT System (Applied Biosystems, Foster City, CA). Relative quantification was performed by the comparative cycle-threshold method (30). The mRNA expression values were normalized to those of the TATA-binding protein gene, used as endogenous control. Statistical analysis of mRNA expression values was performed by Student's *t* test on data normalized to the endogenous controls but not relativized in fold expression of the calibrator sample. Specific real time RT-PCR primers for mouse mRNA primers of *PC4/Tis7*, muscle and cell cycle genes, and of the endogenous controls were deduced from published murine cDNA sequences and are available on request.

Chromatin Immunoprecipitation (ChIP)—ChIP assays were carried out as described, with modifications in the procedure of sample analysis (31). Briefly, cross-linking of C2C12 cells, either infected with shRNA-expressing viruses or not, was performed with 1% formaldehyde for 10 min at room temperature. Then, chromatin was prepared from cell lysates in SDS lysis buffer (1% SDS, 10 mM EDTA, 50 mM Tris-HCl, pH 8) according to standard protocols (Upstate Biotechnology, Inc.). Cellular lysates were sonicated to obtain DNA fragments of average size of 500–700 bp and immunoprecipitated with anti-MyoD antibody (Santa Cruz Biotechnology; rabbit polyclonal M-318 sc-760), or normal rabbit serum as control. The immunoprecipitated DNA and the input DNA were analyzed in duplicate samples by real time PCR using SYBR Green PCR master mix (Applied Biosystems, Foster City, CA) and a 7900HT System (Applied Biosystems).

The amount of immunoprecipitated promoter sequence was calculated as percentage of input (ratio of the average value of the DNA detected in immunoprecipitated samples to the average value of the DNA present in input lysates; as described by Heard *et al.* (32)). For each cell treatment, we calculated in parallel the percentages of DNA immunoprecipitated by immune and normal serum. PCR primers used to amplify were as follows: (*a*) myogenin promoter (region of 140 nt before the transcription start), 5′-GGAATCACATGTAATCCACTGGAAACG-3′ and 5′-GGCTCAGGTTTCTGTGGCGTT-3′; (*b*) muscle creatine kinase (*MCK*) enhancer (region 1100 nt before transcription star; (33)), 5′-GGATGAGAGCAGCCACTACGG-3′ and 5′-CCAGGCATCTCGGGTGTCC-3′; (*c*) *PC4/Tis7* mouse promoter (region 780 nt before transcription start), 5′-TTTGCGACTGTTGATATAACTCATGTATG-3′ and 5′-CAGTTTGGAGGTCAGTTTGGGATAAG-3′; and (*d*) *NeuroD1* promoter, 5′-GTTAGAAGAGGAACTGGAAAGAGAAAGG-3′ and 5′-TGACAGAGGAGGAGGAGGAATGG-3′.

Cell Cycle Analysis—The distribution of cells in the different phases of the cell cycle was studied by using propidium iodide staining. Cells grown as described above were harvested, washed in PBS, fixed in 70% cold ethanol for at least 1 h, and after removing alcoholic fixative, stained with a solution containing 50 μg/ml propidium iodide (Sigma) and 75 KU/ml RNase (Sigma) in PBS, overnight at room temperature in the dark. Twenty thousand events per sample were acquired by using a FACScan cytofluorimeter (BD Biosciences). The percentages of the cell cycle phases were estimated on linear propidium iodide histograms by using the MODFIT software.

Luciferase Assays—C3H10T1/2 fibroblasts (either naive or infected with the retrovirus targeting *PC4*) were transfected with 4RE-LUC, *MCK*-LUC, or the 3×*MEF2*-LUC reporters, whereas C2C12 cells were transfected with the *NF-κB*-LUC reporter and with the indicated expression constructs by using the Lipofectamine reagent. The pRL-*TK* control reporter (*Renilla* luciferase driven by the thymidine kinase promoter) was included in all transfections. 48 h after transfection, luciferase assays were performed by the Dual-Luciferase reporter assay system (Promega) according to the manufacturer's instructions, as described previously (13). The luciferase activity of each sample (Li) was normalized for differences in transfection, measuring in each transfected cell extract the expression levels of *Renilla* luciferase (Ri). The normalized activity of the reporter gene was thus equal to Li × Li/Ri. The fold activity was then obtained by dividing each average normalized reporter activity value by the average normalized reporter activity units of the corresponding control culture. Statistical analysis between groups was performed by Student's *t* test on normalized reporter activity values.

Isolation of Nuclei—Nuclear extracts were obtained from C2C12 cells cultured in GM or 24 and 48 h after shift to DM, following a described protocol, with minor changes (34). Cells were trypsinized and washed in cold phosphate-buffered saline, then the cellular pellet was resuspended in 200 μl of 10 mM HEPES, pH 7.9, 10 mM KCl, 1.5 mM $MgCl_2$, 0.1 mM EGTA, and 0.5 mM dithiothreitol (DTT) on ice. Cells were passed 10 times through a 26-gauge needle and centrifuged to collect nuclei, which were subsequently resuspended in 50 μl of buffer containing 10 mM HEPES, pH 7.9, 0.4 M NaCl, 1.5 mM $MgCl_2$, 0.1 mM EGTA, 0.5 mM DTT, and 5% glycerol. Afterward, nuclei were sonicated and incubated by gentle shaking at 4 °C for 30 min. Finally, nuclear extracts were pelleted at 14,000 rpm for 5 min at 4 °C, and the supernatant was used for electrophoresis. All solutions contained protease inhibitors, 1 mM Na_3VO_4, 10 mM β-glycerophosphate, 10 mM NaF, 5 mM ATP, 5 mM $MgCl_2$, 5 mM sodium butyrate, and 600 nM trichostatin A.

RESULTS

Up-regulation of PC4 in Vivo Stimulates Skeletal Muscle Regeneration—The first question that we sought to address was whether *PC4* was able to positively control skeletal muscle regeneration *in vivo*. To this aim, we generated a bitransgenic mouse model conditionally overexpressing *PC4* in skeletal muscle. We first generated a transgene carrying the coding region of the rat *PC4* cDNA, under the control of tetracycline-responsive elements (TRE, also named TetO by Kistner *et al.* (35)), referred to as TRE-*PC4*. We obtained three transgenic (Tg) TRE-*PC4* mouse family lines (named B, G, and H).

To activate the expression of the *PC4* transgene, the Tg TRE-*PC4* B, G, and H lines were crossed with a second transgenic mouse, *i.e.* CMV-*βactin*-rtTA, carrying the reverse tetracycline transcriptional activator (rtTA) under control of the CMV enhancer/chicken β-actin promoter, whose expression is mainly restricted to skeletal muscle and heart (18). In this way, we obtained three lineages (named B, G, and H) of the bitransgenic mouse CMV-*βactin*-rtTA/TRE-*PC4* (hereafter referred to as Tg *PC4* for brevity), in which doxycycline (a tetracycline analog), administered to mice at the desired time, triggers the production of the transcription transactivator rtTA, which in turn induces the expression of exogenous *PC4* by binding to the TRE within the TRE-*PC4* transgene (Fig. 1*A*).

We monitored the expression of the *PC4* transgene in the adult skeletal muscle of B, G, and H mouse lines of Tg *PC4* at 2 months of age, following administration of doxycycline from P30. It was found that the doxycycline-dependent induction of PC4 protein expression was about 53-, 77-, and 34-fold above basal levels, respectively (as defined by densitometry, after normalization to the total amount of protein per sample; Fig. 1*B*). No evident phenotypic changes in size, weight, viability, and gross morphology were detected in the three Tg *PC4* mouse lines (data not shown). Therefore, the Tg *PC4* line G, showing the highest induction of transgenic PC4 protein in skeletal muscle, accompanied by a very low basal level of expression in the absence of doxycycline, was chosen for further analysis. In Tg *PC4* line G, the transgenic PC4 protein was greatly expressed in skeletal muscle and to a lower level in heart and liver, barely detectable in kidney, and not expressed in brain and spleen (Fig. 1*C*). An analysis of transgenic *PC4* mRNA expression in the Tg *PC4* mouse line G revealed a pattern similar to that of the PC4 protein, with the highest expression in skeletal muscle (Fig. 1*D*, *left panel*); an equivalent level of *PC4* mRNA expression was detected in tibialis anterior, extensor digitorum longus, or diaphragm muscles (*TA*, *EDL*, and *Dia*, respectively; Fig. 1*D*, *right panel*).

Next, we verified whether the up-regulation of *PC4* had any effect on the expression of muscle genes, by measuring their mRNA levels in the TA muscle of P60 bitransgenic Tg *PC4* mice treated with doxycycline since P30. We observed that the activation of the *PC4* transgene (activated Tg *PC4* mice, $n = 4$, and control Tg *PC4* mice, $n = 4$) significantly induced the mRNA levels of *MyoD* and *myogenin* (1.4-fold, $p = 0.03$, and 1.5-fold, $p = 0.01$, respectively; Fig. 2*A*). Moreover, the Tg *PC4*-activated TA muscle showed significantly increased levels of *Pax7* (3-fold, $p = 0.01$), c-*met* (1.6-fold, $p = 0.01$), *nestin* (1.4-fold, $p = 0.01$), and *Myf-5* (3-fold, $p = 0.02$). Finally, *MEF2C* and *MHC* mRNA levels were also induced following doxycycline treatment, although not significantly (1.2-fold, $p = 0.22$, and 1.7-fold, $p = 0.16$, respectively; Fig. 2*A*). Given that *Pax7*, *Myf-5*, c-*met*, and *nestin* are markers of satellite cells (36–38), our results suggest that activation of the *PC4* transgene in adult muscle leads to an increase in the number and/or activity of these cells. Indeed, although mitotically quiescent for much of the time in adult muscle, satellite cells are sporadically activated to proliferate and differentiate to provide new myonuclei for muscle homeostasis and hypertrophy (36). The possibility that the induction of *PC4* can enhance the satellite cell activity is also suggested by the observation that TA muscles from adult (P60) Tg *PC4* mice treated with doxycycline since P30 were found to contain a slightly, although significantly, lower number of myofibers per area than control TA muscles (11% decrease, $p = 0.007$; Fig. 2*B*, *histograms* on the *left*), which implies a larger fiber size.

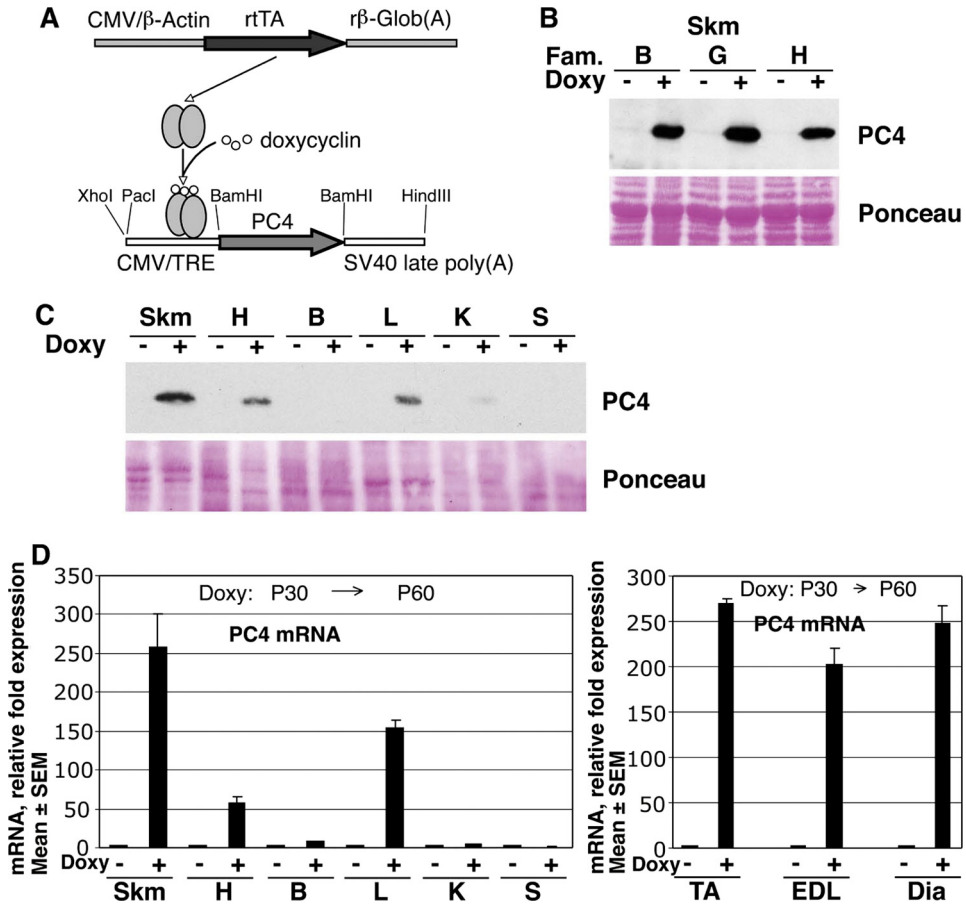

FIGURE 1. **Generation of a conditional bitransgenic mouse expressing *PC4* in skeletal muscle.** *A,* transgene CMV-*β*-*actin*-rtTA contains the CMV enhancer/chicken *β*-actin promoter, followed by the doxycycline rtTA and the rabbit *β*-globin polyadenylation site. The TRE-*PC4* transgene contains TRE fused downstream to the minimal CMV promoter, the *PC4* ORF, and the SV40 late polyadenylation site. The rtTA protein binds the TRE and activates transcription of the *PC4* transgene in the presence of doxycycline. *B,* analysis of the PC4 protein expressed in skeletal muscle by the three lines, B, G, and H, of *PC4* bitransgenic mice, activated or not with doxycycline supplied in the drinking water since P30. *C,* tissue expression analysis of the PC4 protein by Western blot. *D, PC4* mRNA by real time PCR in line G of bitransgenic mice treated or not with doxycycline (*Doxy*). *PC4* mRNA fold expression was calculated relative to the level of expression in untreated mice. Tg *PC4* mice used for experiments were 2 months old and isogenic, being the progeny of at least six generations of interbreeding. *Skm,* skeletal muscle; *H,* heart; *B,* brain; *L,* liver; *K,* kidney; *S,* spleen; *TA,* tibialis anterior; *EDL,* extensor digitorum longum; *Dia,* diaphragm.

Because satellite cells, which are generated during embryonic and fetal muscle development, are mostly active during the early postnatal period to provide myonuclei for skeletal muscle growth (36, 39), we wished also to determine the effects of an earlier induction of *PC4* on satellite cell and myofiber number in adult muscle. To maintain an enhanced expression of *PC4* throughout the time spanning embryonic and postnatal myogenesis until adulthood, we activated Tg *PC4* starting at conception until P45. It turned out that the number of satellite cells per myofiber in TA muscle of P45 Tg *PC4* mice, as determined by quantifying the $Pax7^+$ cells/myofiber, increased significantly with respect to control mice (26% increase, $p = 0.040$; Fig. 2*C*). This effect was accompanied by a significant increase in the number of myofibers per area (29% increase, $p = 0.03$; Fig. 2*B*, *histograms* on the *right*) and a reduction of myofiber cross-sectional area (25% decrease, $p = 0.0001$; supplemental Fig. S1), indicating that a net increase of the total number of satellite cells occurred. As a means to obtain more information about the origin of the *PC4*-dependent increase of satellite cells, we measured also the number of proliferating cells in muscle sections from control and Tg *PC4* mice activated since conception, at the age P10, P15, and P30. Proliferating muscle cells were labeled by injecting mice intraperitoneally with BrdU daily for 4 days preceding the day of analysis. In Tg *PC4* mice, we observed a significant increase of BrdU-positive nuclei per myofiber at P10 (36% increase, $p = 0.04$; supplemental Fig. S2, *A* and *B*), and a less pronounced increase at P15 and at P30. These data suggest an enhancement by PC4 of satellite cells activity during the early postnatal life and, altogether, are consistent with the idea that *PC4* up-regulation leads to enhanced myogenesis.

Next, we sought to assess the effects of *PC4* up-regulation on the process of muscle regeneration during adulthood, *i.e.* independently from any effect on embryonic/postnatal myogenesis. To this aim, we lesioned the TA muscle by cardiotoxin injection in P60 Tg *PC4* bitransgenic mice exposed to doxycycline since P30, and we quantified the number of regenerating fibers in time course experiments. Throughout all the experiments with the bitransgenic Tg *PC4* mouse line, we used as control mice the progeny that did not inherit the TRE-*PC4* transgene. This protocol also allowed the treatment of control mice with doxycycline, thus equalizing any possible effect on regeneration of doxycycline itself. The myofibers

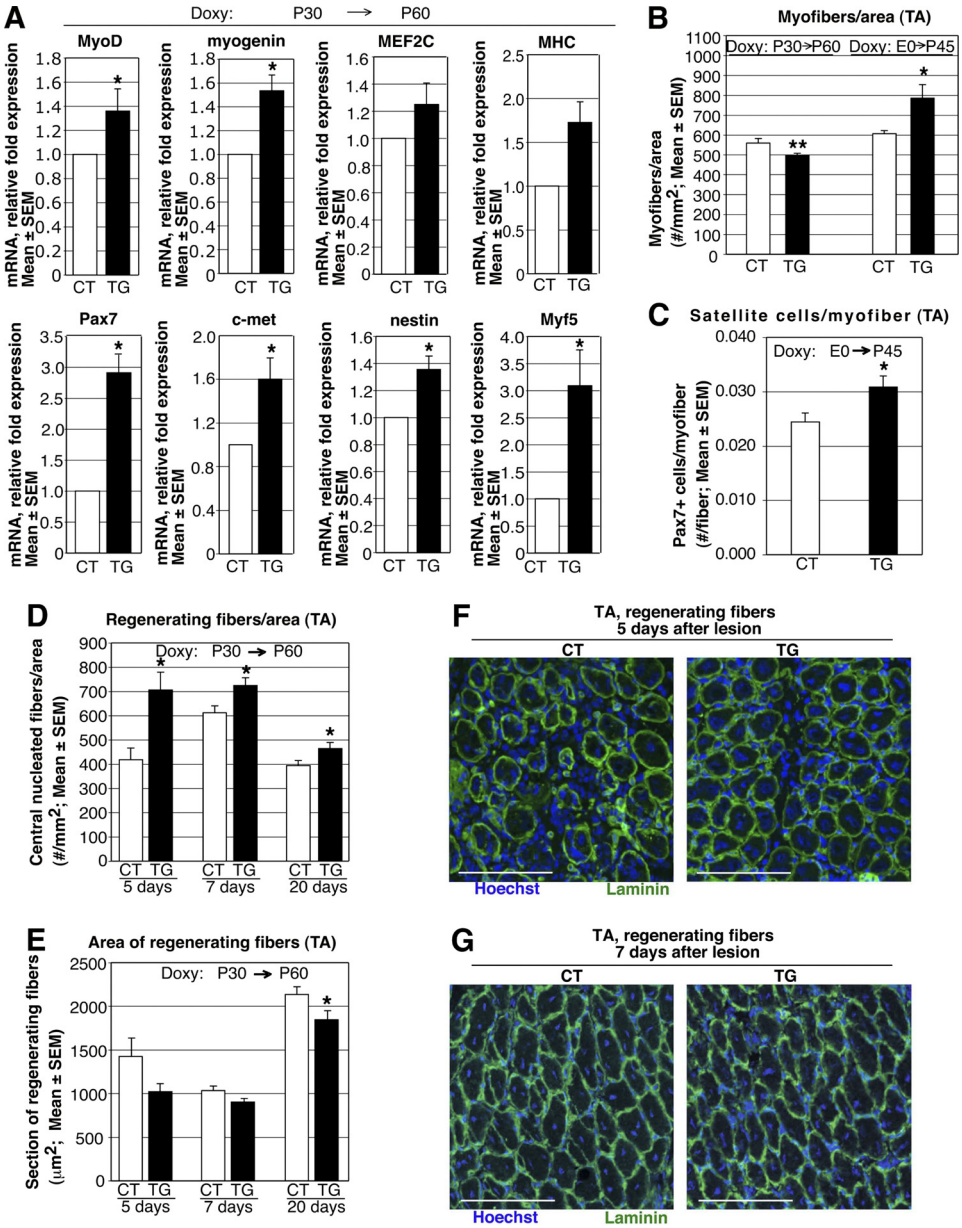

FIGURE 2. ***PC4* up-regulation in skeletal muscle increases myogenic gene expression and satellite cells number and potentiates regeneration.** *A,* induction of *MyoD, myogenin, MEF2C, MHC, Pax7, c-met, nestin,* and *Myf5* mRNA levels in TA muscle from 2-month-old Tg *PC4* mice with transgene activated since P30 (TG), relative to control mice (*CT*). $n = 3$ for each group. *B,* decrease of the number of myofibers per area in cross-sections of TA from P60 Tg *PC4* mice with transgene activated since P30 (*left*); increase of the number of myofibers per area in TA of P45 Tg *PC4* mice with transgene activated since conception (*right*). *C,* increase of the number of satellite cells, measured as $Pax7^+$ cells/myofiber in cross-sections from TA muscle of P45 Tg *PC4* mice with transgene activated since conception. The experiments shown in *B* and *C* were performed with $n = 3$ animals for both CT and TG groups. *D,* increase of the number of regenerating myofibers in TA muscle of P60 Tg PC4 mice with transgene activated at P30, identified by the presence of central nuclei. Injury was induced by injecting cardiotoxin in TA 5, 7, and 20 days before killing mice at P60 for analysis. *E,* cross-sectional area of regenerating myofibers analyzed in *D* showed a decrease in Tg *PC4* mice that became significant in the 20 days post-lesion group. $n = 3$ for CT and $n = 4$ for TG groups 5 and 7 days post-lesion; $n = 3$ for both CT and TG groups 20 days post-lesion. *, $p < 0.05$, or **, $p < 0.01$ CT *versus* the Tg PC4 mice group, Student's *t* test. *F* and *G,* representative confocal microscopy images of the regenerating myofibers at 5 and 7 days after injury, respectively. Immunofluorescence staining for laminin was used to identify the basal lamina surrounding each myofiber; nuclei were visualized by Hoechst 33258. *Bar* indicates 100 μm. *A–G,* CT mice were bitransgenic mice that did not inherit the TRE-*PC4* transgene, exposed to doxycycline (*Doxy*) as the activated bitransgenic mice (TG).

were identified by immunofluorescence staining with anti-laminin antibody, and the nuclei having central localization, an hallmark of regenerating myofibers, were detected by Hoechst 33258. We observed that the lesioned TA muscle of Tg *PC4* mice, at 5, 7, and 20 days after injury presented a number of centrally nucleated myofibers per area significantly higher than the lesioned muscle from control mice (5 days post-lesion: control $n = 3$, Tg *PC4* $n = 4$, $p = 0.016$; 7 days post-lesion: control $n = 3$, Tg *PC4* $n = 4$, $p = 0.011$; 20 days post-lesion: control $n = 3$, Tg *PC4* $n = 3$, $p = 0.03$; Fig. 2, *D*, *F,* and *G*). Consistently, the average cross-sectional area of regenerating fibers, measured in parallel in the same sections, presented in Tg *PC4* mice a tendency to decrease, with a difference from control that attained statistical significance 20 days after the lesion (5 days post-lesion, $p = 0.06$; 7 days post-lesion, $p = 0.06$; 20 days post-lesion, 13% decrease, $p =$

0.02; n = as indicated above; Fig. 2, *E–G*). As a whole, these data indicate that the capability of adult muscle to generate new myofibers following acute damage was significantly potentiated by up-regulation of *PC4*.

RNAi Knockdown of PC4 in Myoblasts Leads to Inhibition of Muscle Differentiation Genes and Induction of Cyclins—The above data establish that *PC4* acts as enhancer of postnatal and regenerative myogenesis but do not ascertain the underlying mechanism. To achieve this goal, we first considered it appropriate to extend previous analyses on the effects of *PC4* deprivation on myoblast differentiation. We targeted *PC4* by RNA interference in the C2C12 myoblast cell line, which was originally derived from satellite cells isolated from adult muscle (40). To identify a retrovirally delivered short hairpin RNA (shRNA) specifically targeting *PC4*, we analyzed several candidate 19-nt *PC4* targeting sequences designed by the MWG on-line Design Tool software (MWG, Ebersberg, Germany). The various sequences were cloned in the pSUPER.retro vector, and the corresponding retroviruses were produced in the Phoenix helper cells. C2C12 myoblasts were then infected with retroviruses expressing the different *PC4* targeting sequences or with the insertless control retrovirus and selected for resistance to puromycin. The analysis of the derived myoblast populations identified two shRNA sequences capable of silencing PC4 protein expression, albeit with different efficiencies, named RS/2 and RS/7 (Fig. 3*A*). Myoblasts infected with RS/2 or RS/7 retroviruses presented in both cases inhibition of MHC expression in cultures kept 48 h in DM, to an extent proportional to the silencing of endogenous *PC4* exerted by each shRNA.

RS/2 shRNA, which inhibited almost completely the expression of endogenous PC4 protein both in proliferating and differentiating myoblasts, was chosen for further experiments. C2C12 myoblasts infected with RS/2 retrovirus also displayed inhibition of endogenous *PC4* mRNA, as determined by Northern analysis (Fig. 3*B*).

In first place, we tested the effect of *PC4* silencing on the morphological differentiation of C2C12 myoblasts. It turned out that the number of cells expressing the late differentiation marker MHC after 72 h in DM was reduced about 40% (see Fig. 3*C*, and differentiation index, Fig. 3*D*; $p < 0.002$). In the absence of *PC4*, myoblasts in DM attained an elongated phenotype but were unable to fuse into multinucleated myotubes (Fig. 3*D*); the fusion index was indeed reduced by more than 50% (Fig. 3*E*; $p < 0.0002$).

An expression analysis of several muscle and cell cycle regulatory proteins was then carried out in C2C12 myoblasts infected with the retrovirus expressing the *PC4*-targeting shRNA, as compared with control myoblasts infected with the empty retrovirus. *PC4*-deprived myoblasts expressed reduced levels of the myogenic regulatory factors MyoD and Pax7 both in GM and DM, respectively, and accumulated decreased levels of early (myogenin, MEF2C) and late muscle proteins (sarcomeric α-actin and MHC; Fig. 4, *left panel*). In contrast, the expression of Myf-5 was induced in differentiating myoblasts lacking PC4. (Fig. 4, *left panel*). We further verified that the shRNA-dependent decrease of muscle genes was specific to the *PC4* targeting sequence, as the pSUPER retrovirus carrying an shRNA sequence targeting luciferase did not inhibit MyoD or MHC levels, similarly to what observed with the insertless virus (supplemental Fig. S3). As for the effects on cell cycle regulatory proteins, *PC4*-deprived myoblasts displayed higher levels of cyclin D1 in proliferating conditions (GM), as well as during the first 24 h in DM compared with control myoblast cultures. Also, cyclin A and cyclin E levels increased in *PC4*-depleted differentiating myoblasts, albeit less evidently than those of cyclin D1, and the retinoblastoma protein (pRb) showed a delayed kinetics of dephosphorylation. However, 48 h after the onset of differentiation, the expression of cell cycle genes attained control levels. No evident change was detected for cyclin D3 and p21 (Fig. 4, *right panel*). Together, these data indicate that *PC4*-deprived, differentiating myoblasts remain in the cell cycle for a longer period and are impaired in their terminal differentiation, as compared with control myoblasts.

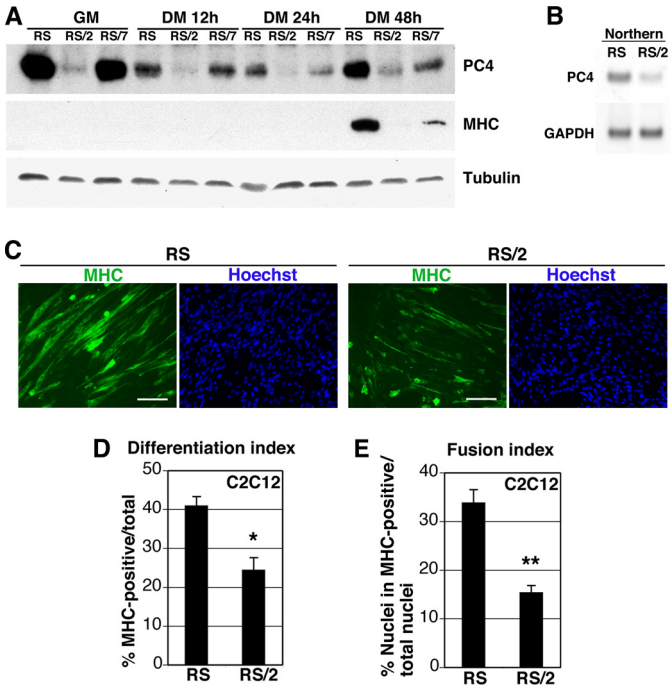

FIGURE 3. **shRNA-mediated inhibition of *PC4* expression impairs myoblast differentiation.** *A,* analysis of PC4 and myosin heavy chain (*MHC*) protein expression in proliferating (GM) or differentiating (DM) C2C12 myoblasts, infected with retroviruses generated by the pSUPER-retro vector expressing the *PC4*-specific shRNA sequences *PC4*/2 and *PC4*/7 (RS/2 and RS/7, respectively) or with the insertless retrovirus (*RS*). After infection, cells were selected for 96 h with puromycin and then cultured in proliferating (GM) or differentiating conditions (DM), as indicated. *B,* Northern analysis of C2C12 myoblasts infected with the retrovirus expressing *PC4* shRNA (*RS/2*) or with the insertless control retrovirus (*RS*). Total RNA was analyzed with a ^{32}P-labeled *PC4* or *GAPDH* probe, as a measure of the amount and integrity of the mRNA. *C,* C2C12 myoblasts, infected with the retrovirus expressing *PC4* shRNA (*RS/2*) or with the insertless control retrovirus (*RS*), were cultured in DM for 96 h; cells were then fixed and stained for immunofluorescence detection with anti-MHC antibody through secondary goat anti-rabbit FITC-conjugated antibody. Nuclei were detected by Hoechst 33258 dye (corresponding photomicrographs on the *right*). *Bar,* 140 μm. RS/2-infected cultures show a clear impairment of differentiation. Differentiation index (percentage of cells labeled by MHC) (*D*) and fusion index (percent ratio of the number of nuclei detected in MHC-labeled cells to the total number of nuclei) (*E*) were both significantly decreased. The numbers of myoblasts analyzed were 2067 and 1920 for RS- or RS/2-infected cultures, respectively. *, $p < 0.01$; **, $p < 0.001$, Student's *t* test.

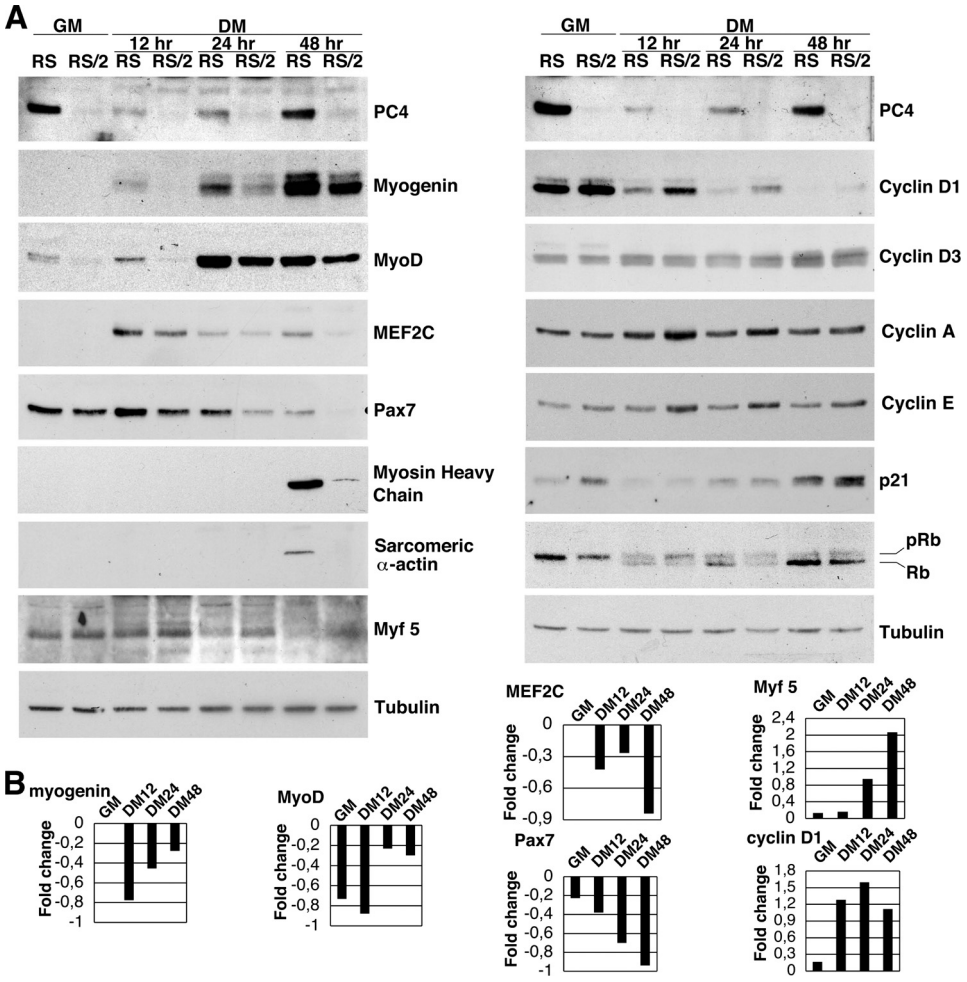

FIGURE 4. **Inhibition of muscle-specific proteins and induction of cell cycle proteins following deprivation of *PC4* in myoblasts.** *A,* expression analysis of the indicated muscle and cell cycle proteins in proliferating or differentiating C2C12 myoblasts deprived of *PC4*. Representative Western blots are shown (out of a total of three experiments). Myoblast cultures infected with the retrovirus expressing the *PC4*-targeting RS/2 shRNA or with the insertless retrovirus were selected with puromycin for 96 h and then cultured in GM or in DM for the indicated times. *B,* densitometry analysis of Western blots is shown in *A*; values are presented as fold change of protein expression in *PC4*-deprived cells relative to RS control cells, after normalization to the corresponding values of α-tubulin expression (the control base line is set to 0).

Next, we defined whether the effects elicited by *PC4* silencing occurred at the mRNA level by measuring the transcripts of muscle and cell cycle genes in C2C12 differentiating myoblasts expressing shRNA against *PC4*, compared with control myoblasts. We observed that in the absence of *PC4*, the mRNA expression of all muscle genes analyzed (*myogenin*, *MyoD*, *MEF2C*, *Pax7*, *MHC*, and *MCK*) was significantly inhibited throughout differentiation, with the exception of *Myf-5*, similarly to what was observed for protein levels (Fig. 5). In contrast, the mRNA levels of cell cycle genes were higher in myoblasts deprived of *PC4*, with a significant increase of cyclin D1 transcripts in proliferating as well as in differentiating myoblasts; such an effect, although less pronounced, occurred also for cyclin E and, to a lesser extent, for cyclin A (Fig. 5).

PC4 Deprivation Delays the Exit from Cell Cycle at the Onset of Differentiation by a MyoD-dependent Mechanism—The above results showed that *PC4* silencing in proliferating myoblasts was associated to an evident inhibition of *MyoD* and *Pax7* expression and to a concomitant increase of cyclin D1 and cyclin E levels (Figs. 4 and 5). This raised the question as to whether the absence of *PC4* affects the cell cycle genes directly or as the consequence of a primary effect on differentiation-controlling genes.

Therefore, we sought to analyze the cell cycle profile of proliferating or differentiating myoblasts lacking *PC4*, as compared with control myoblasts. No significant differences emerged between control and *PC4*-depleted proliferating (GM) myoblast populations with regard to the relative abundance of cells in the G_0/G_1, S, or G_2/M phases of the cell cycle (Fig. 6*A*). This suggests that the deprivation of *PC4* does not affect cell cycle progression. Nonetheless, when the relative abundance of G_0/G_1, S, or G_2/M phase cell populations was analyzed in differentiating cells, it turned out that in the absence of *PC4* the number of cells in the G_0/G_1 phase was significantly reduced after 12 or 24 h in differentiation medium, whereas in parallel, the S phase population was highly increased (Fig. 6*A*). Such increase of the S phase cell population became less evident after 48 h in differentiation medium. As a whole, this indicates that the progressive exit from the cell cycle was significantly delayed in differentiating myoblasts lacking *PC4.*

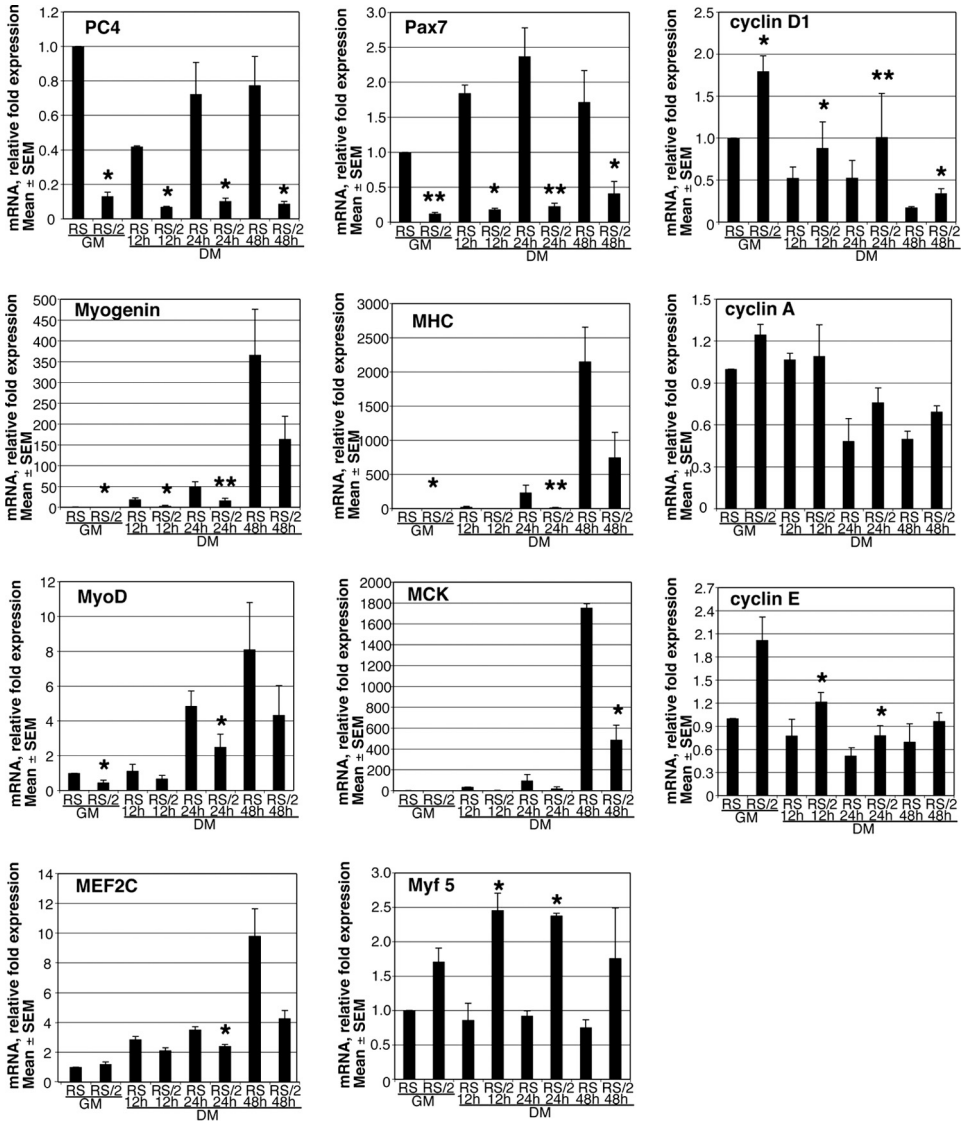

FIGURE 5. **Deprivation of *PC4* results in inhibition of muscle gene mRNA expression and enhanced expression of cell cycle genes.** Real time PCR analysis of the indicated muscle and cell cycle mRNAs from C2C12 myoblasts, infected with the retrovirus expressing the shRNA to *PC4* (RS/2) or with the control retrovirus (*RS*). Cells were cultured in GM or DM as indicated. Average ± S.E. values are from three independent experiments and are shown as fold change relative to control sample (RS-infected cells in GM), which was set to unit. TATA-binding protein mRNA was used as endogenous control for normalization. *, $p < 0.05$; **, $p < 0.01$ *versus* the corresponding time point of control-infected cells (RS), Student's *t* test.

This conclusion is consistent with the increased levels of cyclin D1 and cyclin E, which regulate the transition from G_1 to S phase (41, 42), observed in myoblasts lacking *PC4* 12 and 24 h after the shift to DM (Fig. 4). As MyoD is known to limit cell cycle progression by promoting G_1 arrest (43, 44), we asked whether the prolonged permanence in the cell cycle of *PC4*-deprived differentiating myoblasts was primarily due to the impaired expression of MyoD in these cells.

To this end, we analyzed the effect of *PC4* deprivation in C3H10T1/2 fibroblasts, either in the absence or in the presence of retrovirally transduced exogenous *MyoD* (Fig. 6, *B* and *C*). We found that in the absence of *PC4*, C3H10T1/2 fibroblasts transduced with *MyoD* showed a significant reduction of the cell population in G_0/G_1 phase 12 h after the shift to DM, although the S phase cell population was significantly increased at the same time point (Fig. 6*B*). This result is similar to that obtained in differentiating C2C12 cells (see above Fig. 6*A*). In contrast, no significant effect of *PC4* deprivation was observed in the absence of MyoD on the relative abundance of cell populations in G_1-S-G_2/M in differentiation medium (Fig. 6*C*). This suggests that the delayed exit from cell cycle of *PC4*-deprived myoblasts occurs as the consequence of *MyoD* down-regulation.

PC4 Silencing Impairs the MyoD/MEF2 Transcriptional Function—It is known that *MyoD* can positively regulate its own expression through an autoregulatory loop also involving the activity of MEF2 factors, which in turn are activated by MyoD (45, 46). Our previous data indicate that the overexpression of *PC4* potentiates the activity of *MyoD* by promoting the transcriptional function of MEF2C (13). However, key points still undefined are whether *PC4* is necessary for the activity of *MyoD* and *MEF2C* and whether there are additional pathways responsible for the action of *PC4*.

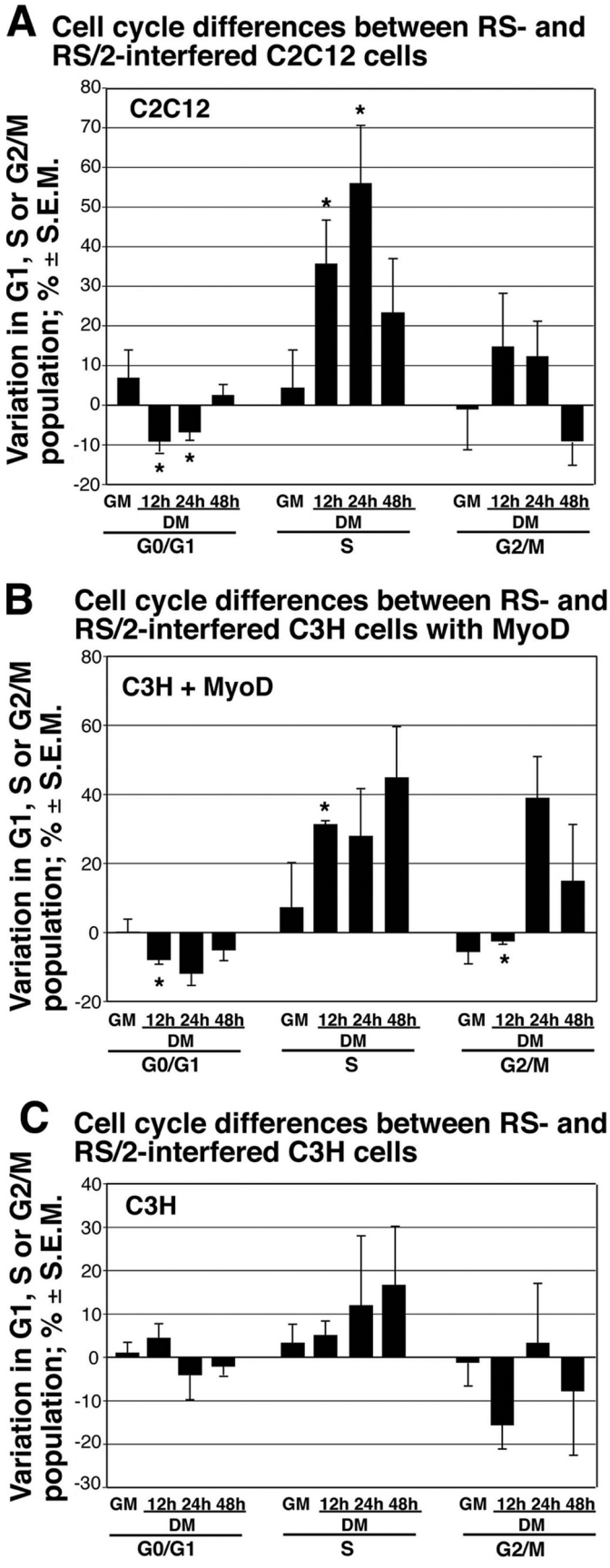

FIGURE 6. **MyoD-dependent delay of cell cycle exit in C2C12 myoblasts deprived of *PC4*.** *A,* flow cytometry analysis of proliferating or differentiating C2C12 myoblasts infected with the retrovirus expressing shRNA to *PC4* (*RS/2*) or with the control retrovirus (*RS*). The infected cells were selected with puromycin for 96 h and then cultured in GM or DM for the indicated times. The DNA content was analyzed after staining with propidium iodide, by flow cytometry. Data from five independent experiments are shown as means ± S.E. of the changes in the percentage of *PC4*-silenced cells in G_0/G_1, S, or G_2/M cycle phase, relative to the percentage of cells infected with the control virus. RS/2-infected cells show a significant decrease of the G_1, and an increase of the S population, 12 and 48 h after shift to DM. *, $p < 0.05$ *versus* the corresponding control group at the same time point, Student's *t* test. *B* and *C,* flow cytometry analysis of C3H10T1/2 fibroblasts deprived of *PC4*, induced or not to differentiate into myotubes by ectopic MyoD. C3H10T1/2 cell cultures were infected with PC4-targeting shRNA retrovirus (*RS/2*) or with control retrovirus (*RS*), selected with puromycin for 96 h, and then infected with a retrovirus expressing *MyoD* (pBABE-*MyoD*) (*B*), or infected with the control retrovirus (pBABE) (*C*). Infected cells were cultured in GM or DM as indicated. Data from three independent experiments are shown as means ± S.E. of the changes in the percentage of *PC4*-silenced cells in the different cell cycle phases, with respect to control cells. The absence of *PC4* causes cell cycle changes similar to those observed in C2C12 myoblasts only in C3H10T1/2 cells expressing *MyoD*. *, $p < 0.05$ *versus* the corresponding control group (RS-infected) of the same time point, Student's *t* test.

Thus, to test if the absence of *PC4* results in an inhibition of MyoD and MEF2 activity, reporter assays were performed in C3H10T1/2 fibroblasts expressing shRNA targeting *PC4* or in control fibroblasts, cotransfected with increasing amounts of an expression construct for MyoD (pCDNA3-FLAG-*MyoD*) and either the 4RE-LUC reporter, carrying four tandemly repeated MyoD binding sites, the *MCK*-LUC reporter, carrying *MCK* enhancer sequences containing both MyoD and MEF2-binding sites, or the 3×MEF2-LUC reporter, carrying three tandemly repeated *MEF2* sites (Fig. 7, *A–C*). It was found that the RNAi-mediated knockdown of *PC4* significantly inhibited the MyoD-mediated transactivation of all tested reporters (4RE-LUC reporter, $p = 0.04$ and 0.01; *MCK*-LUC reporter, $p = 0.02$ and 0.02; 3×*MEF*2-LUC reporter, $p = 0.04$ and 0.004, for 0.1 or 0.2 μg of cotransfected *MyoD*, respectively). However, examination of whole-cell lysates and total RNA from these transfections indicated that deprivation of *PC4* reduced both the mRNA and protein levels of the exogenous FLAG-tagged *MyoD* (Fig. 7, *D* and *E*). This unexpected evidence, although preventing us from answering specifically the initial question as to whether the transcriptional activity of MyoD was inhibited in the absence of *PC4*, revealed that PC4 may stimulate *MyoD* mRNA accumulation, which may represent a novel function of *PC4* (see below).

Furthermore, given that our previous data demonstrated that PC4 coactivates MyoD by enhancing the activity of MEF2C (13), we wished to test whether the RNAi-mediated knockdown of *PC4* could directly affect the transcriptional activity of MEF2C, independently of any effect on *MyoD*. To this aim, we performed reporter assays in C2C12 myoblasts, cultured in proliferating conditions where MyoD is inactive. Myoblasts expressing shRNA to *PC4* or control myoblasts were cotransfected with the MEF2-responsive reporter construct and vectors expressing *MEF2C* and *PC4* or *MEF2C* alone. We observed that the silencing of *PC4* significantly reduced the transactivation mediated by MEF2C alone, as well as that potentiated by PC4 ($p = 0.043$ and $p = 0.008$, respectively; Fig. 7, *F* and *F*′). To further test whether *PC4* could directly control the activity of MEF2C, we cotransfected the *MEF2*-responsive reporter and an expression construct for

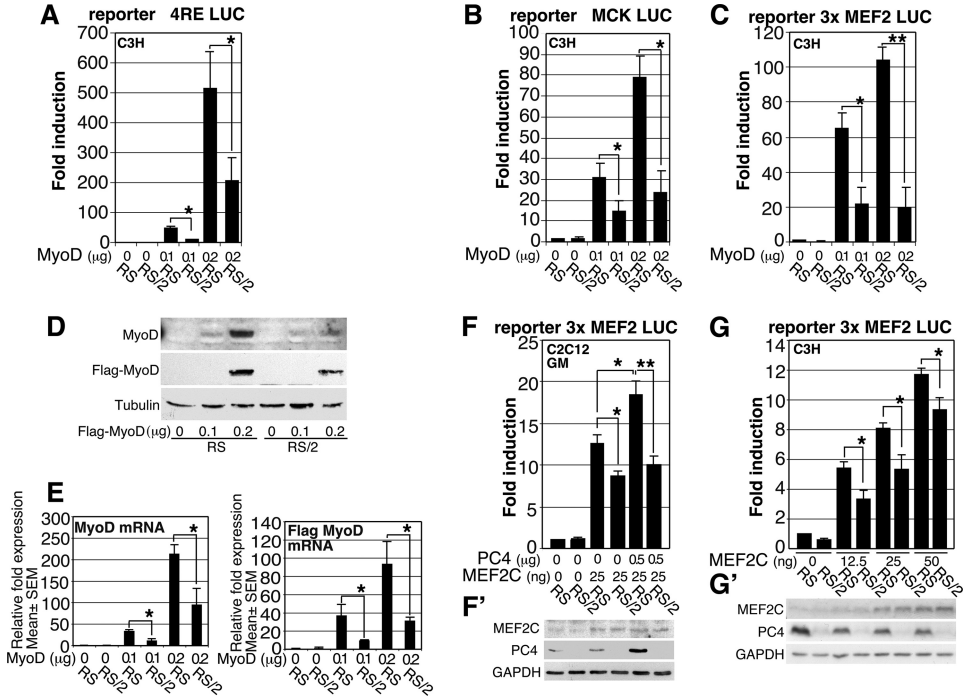

FIGURE 7. **Reduced transcriptional activity of MyoD and MEF2C in the absence of *PC4*.** *A–C,* C3H10T1/2 cell cultures were infected with the shRNA retrovirus expressing shRNA to *PC4* (*RS/2*) or the control retrovirus (*RS*); following selection with puromycin for 96 h, cells were seeded in 35-mm dishes (7×10^5) and cotransfected the next day with the pCDNA3-FLAG-*MyoD* construct (0.1 or 0.2 μg) or the empty vector and either the 4RE-LUC reporter (0.1 μg) (*A*), *MCK*-LUC reporter (0.3 μg) (*B*), or 3×MEF2-LUC reporter (0.2 μg) (*C*). After 24 h, the cultures were shifted to DM and harvested for analysis 48 h later. Luciferase (*LUC*) activity from cell extracts was expressed as fold induction relative to the activity of the RS-infected control sample not transfected with *MyoD* (that was set to unit), and it resulted in significantly reduced cultures deprived of PC4, with respect to control RS cultures. *Bars* represent the average fold induction ± S.E. determined in four independent experiments, each performed in duplicate. *, $p < 0.05$ or **, $p < 0.01$ (Student's *t* test). Parallel C3H10T1/2 cell cultures treated as above were analyzed for endogenous and exogenous MyoD protein expression by Western blot (*D*) and for *MyoD* mRNA expression by real time PCR (*E*), which is shown as average ± S.E. fold expression relative to the RS-infected control sample not transfected with MyoD, set to unit. TATA-binding protein mRNA was used as endogenous control for normalization. *, $p < 0.05$ (Student's *t* test). *F,* C2C12 cells infected with the RS/2 retrovirus targeting *PC4* or the control RS retrovirus were plated in duplicate in 35-mm culture dishes (5×10^4) and cotransfected the following day with the 3×*MEF2*-LUC reporter (0.1 μg), the pCDNA1-*MEF2C* (0.025 μg), and the pSCT-*PC4* (0.5 μg) expression vectors, as indicated. Cells were maintained in GM and harvested 48 h after transfection. Luciferase activities are expressed as fold induction relative to the activity of the RS-infected control sample not transfected with *MEF2C* or *PC4*. *Bars* represent the average fold induction ± S.E. from three independent experiments performed in duplicate. *, $p < 0.05$; **, $p < 0.01$ (Student's *t* test). *F′*, parallel cultures were analyzed for MEF2 protein expression by Western blot. *G,* C3H10T1/2 cells infected with the RS/2 or the control RS shRNA retroviruses were transfected with the 3×*MEF2*-LUC reporter (0.1 μg) and increasing concentrations of pCDNA1-MEF2C expression vector, as indicated. Cells were maintained in GM and harvested 48 h after transfection. Luciferase activities are expressed as fold induction relative to the activity of the RS-infected control sample. *Bars* represent the average fold induction ± S.E. from four independent experiments performed in duplicate. *, $p < 0.05$ (Student's *t* test). *G′*, parallel cultures were analyzed for MEF2 protein expression by Western blot.

MEF2C in C3H10T1/2 cells, which do not express *MyoD*, where *PC4* had been silenced or not. It turned out that the absence of *PC4* caused a significant reduction of the activity of the *MEF2*-responsive reporter at increasing concentrations of *MEF2C* ($p = 0.002$, $p = 0.003$ and $p = 0.004$, respectively; Fig. 7, *G* and *G′*). Therefore, the data of Fig. 7 show that the absence of *PC4* can directly impair the transactivating activity of MEF2C.

PC4 Inhibits the Activity of NF-κB by Inducing HDAC-dependent Deacetylation of p65—The above results indicated that the *PC4* silencing inhibited the levels of *MyoD* transcript in C2C12 cells (Fig. 5), as well as the MyoD levels produced from a transfected expression construct under the control of a heterologous promoter (Fig. 7, *D* and *E*). This suggested that *PC4*, besides regulating *MyoD* transcription through MEF2C, might be implicated also in a second mechanism controlling *MyoD* mRNA accumulation. Noteworthy, it has been shown that NF-κB can suppress *MyoD* expression at the post-transcriptional level through a destabilization element in the *MyoD* transcript (47). This observation raised the intriguing hypothesis that *PC4* could have an impact on *MyoD* through *NF-κB*. Thus, we investigated a possible functional interaction between PC4 and NF-κB by analyzing in C2C12 cells the effect of an overexpression or deprivation of PC4 on the transactivation potential of NF-κB. To this aim, a luciferase reporter gene fused to two tandem repeats of the κB site (2×NF-κB-LUC (48)) was transfected in C2C12 myoblasts with or without an expression vector for *PC4,* and its activity was measured in proliferating conditions (GM) or after 48 h in differentiating conditions (DM; Fig. 8*A*). We observed that the overexpression of *PC4* significantly inhibited the endogenous activity of *NF-κB*, both in proliferating and in differentiating myoblasts ($p = 0.02$ for both conditions; Fig. 8*A*, *left*). Moreover, *PC4* overexpression was also able to inhibit significantly the tumor necrosis factor α (TNF)-induced activity of *NF-κB* in proliferating but not in differentiating conditions ($p = 0.04$ and $p = 0.11$, respectively; Fig. 8*A*, *right*). The expression of equal levels of PC4 protein produced under the corresponding conditions (*i.e.* GM and DM) by the transfected *PC4* expression construct was checked by Western blot

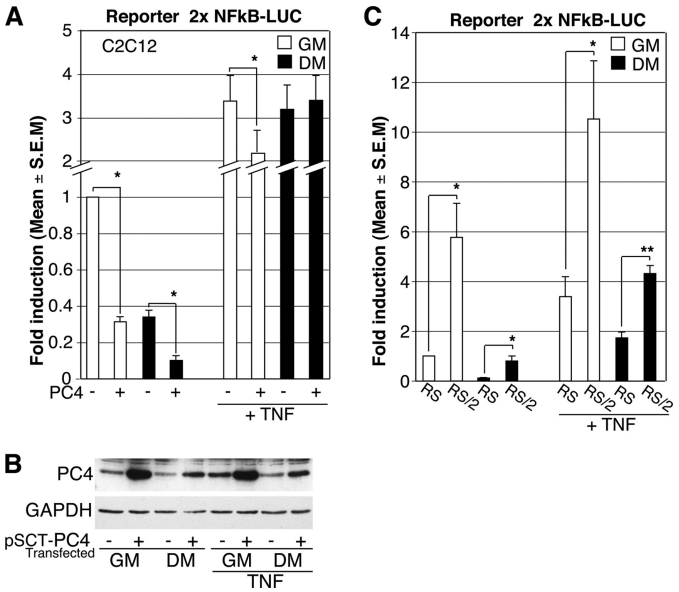

FIGURE 8. **PC4 represses the NF-κB transactivation function.** *A,* C2C12 cells were plated in duplicate 35-mm culture dishes (7×10^4 cells) and co-transfected the next day with the *NF-κB*-LUC reporter (0. 1 μg) and either the pSCT-*PC4* expression construct or the empty pSCT vector (0.5 μg). Cells were either maintained in GM or switched to DM 24 h after transfection and harvested 48 h later. TNF (10 ng/ml) was added 6 h before harvesting, where indicated. Luciferase activity from cell extracts is expressed as fold induction relative to the activity of the GM control sample (transfected with the empty vector and not treated with TNF). *Bars* represent the average fold induction ± S.E. determined from five independent experiments, each performed in duplicate. *, $p < 0.05$ (Student's *t* test). *B,* C2C12 cells transfected as in *A* were analyzed for PC4 protein expression by Western blot. *C,* C2C12 cells infected with the RS/2 retrovirus expressing shRNA to *PC4* or the control retrovirus (*RS*) were plated in duplicate 35-mm culture dishes (7×10^4 cells) and transfected the next day with the NF-κB-LUC reporter (0.1 μg). Cells were either maintained in GM or switched to DM 24 h after transfection and harvested 48 h later; where indicated, TNF (10 ng/ml) was added 6 h before harvesting. Luciferase activity is expressed as fold induction relative to the activity of the GM RS-infected control sample not treated with TNF. *Bars* represent the average fold induction ± S.E. determined from five independent experiments performed in duplicate. *, $p < 0.05$; **, $p < 0.01$ (Student's *t* test).

(Fig. 8*B*). Conversely, C2C12 myoblasts where the expression of *PC4* had been silenced by shRNA presented a significant stimulation of *NF-κB* activity both in proliferating and differentiating conditions ($p = 0.02$ and $p = 0.01$, respectively; Fig. 8*C*, *left*), also following stimulation by TNF ($p = 0.049$ in GM; $p = 0.005$ in DM; Fig. 8*C*, *right*). These findings reveal that *PC4* can function as a negative regulator of NF-κB transcriptional activity.

NF-κB consists of five members, RelA(p65), RelB, c-Rel, p50, and p52, that form homo- and heterodimers, with the p65/p50 complex being the most common. In inactive conditions, NF-κB is bound to IκB inhibitor proteins that mask its nuclear translocation signal and sequester it in the cytoplasm (49). Following phosphorylation of IκBα by IκB kinase, the p65/p50 dimers are released from IκBα and translocate to the nucleus (50, 51). The concomitant acetylation of p65 by P300/CBP acetyltransferases prevents its reassociation with the IκBα inhibitor and the ensuing nuclear export (52, 53). Therefore, the acetylation state of p65 critically controls the nuclear localization, and hence the activity, of p65. It has been shown that the p65 subunit of NF-κB is constitutively present in the nuclei of proliferating myoblasts, whereas nuclear p65 levels decline during their differentiation (54). Given that the deacetylation of p65 mediated by HDACs negatively modulates the activity of NF-κB (52, 55), and we and others demonstrated that PC4 binds HDACs (13, 56), we sought in the first place to assess whether *PC4* could enhance the HDAC-mediated inhibition of *NF-κB* activity in proliferating myoblasts. We observed that *PC4* significantly potentiated the inhibition exerted by *HDAC4* or *HDAC3* of the endogenous activity of *NF-κB* ($p < 0.05$ for both *HDACs*; Fig. 9, *A* and *B*). The amount of proteins produced by the transfected *PC4*, *HDAC4*, and *HDAC3* expression constructs was checked by Western blot (Fig. 9, *A′* and *B′*). Next, we determined by Western blot analysis of nuclear extracts the levels of nuclear p65 and its state of acetylation in proliferating or differentiating myoblasts lacking *PC4*, compared with control myoblasts. The levels of c-Jun were also determined to normalize for nuclear protein amounts, whereas those of cytoplasmic glyceraldehyde-3-phosphate dehydrogenase (GAPDH) served as control for purity of nuclear extracts (Fig. 9*C*). It was found that *PC4*-deprived myoblasts displayed increased levels of nuclear p65, acetylated in lysine 310, in either culture condition, although most evidently in proliferating myoblasts, which was accompanied by down-regulation of MyoD levels (Fig. 9*C*). This finding, together with the above reported ability of PC4 to synergize with HDACs in inhibiting NF-κB activity, strongly suggests that PC4 negatively regulates through HDACs the acetylation state of p65 and consequently its activity and localization. Notably, acetylation of p65 at lysine 310 is thought to be necessary for the full transactivation function of p65 (57).

We further checked the ability of PC4 to control the acetylation state of p65 in primary myoblasts freshly isolated from the adult muscle of Tg *PC4* mice at P45. The expression of the *PC4* transgene was induced *in vivo* since conception and was kept active in cultured myoblasts. We found that the up-regulation of *PC4* led to a decrease of nuclear p65 acetylated in lysine 310 in proliferating primary myoblasts (although in differentiating myoblasts acetylated p65 was not detectable, given the very low levels of p65 in this condition). Concomitantly, we observed an increase of MyoD levels. This result confirms that PC4 exerts a negative control on p65 acetylation and hence on its activity, in correlation with an induction of MyoD expression, and suggests that such action is effective *in vivo* (Fig. 9*D*).

Finally, we sought to investigate whether PC4 can form molecular complexes with p65 and HDAC3. To this aim, lysates of C2C12 myoblasts (clone S4 constitutively overexpressing PC4; Ref. 13) transfected with *myc-HDAC3* were immunoprecipitated with the anti-p65 antibody and subjected to Western blot analysis with an anti-PC4 antibody or with an anti-Myc antibody to reveal HDAC3. As shown in Fig. 9*E*, PC4 was found to associate with p65 in complexes also containing HDAC3, both in proliferation and in differentiation conditions (*i.e.* GM and DM). This result suggests the possibility that PC4 may stimulate p65 deacetylation by facilitating the recruitment of HDAC3 to p65.

MyoD Binds to the PC4 Gene Promoter—In a previous study, we have shown that the expression of *MyoD* in fibro-

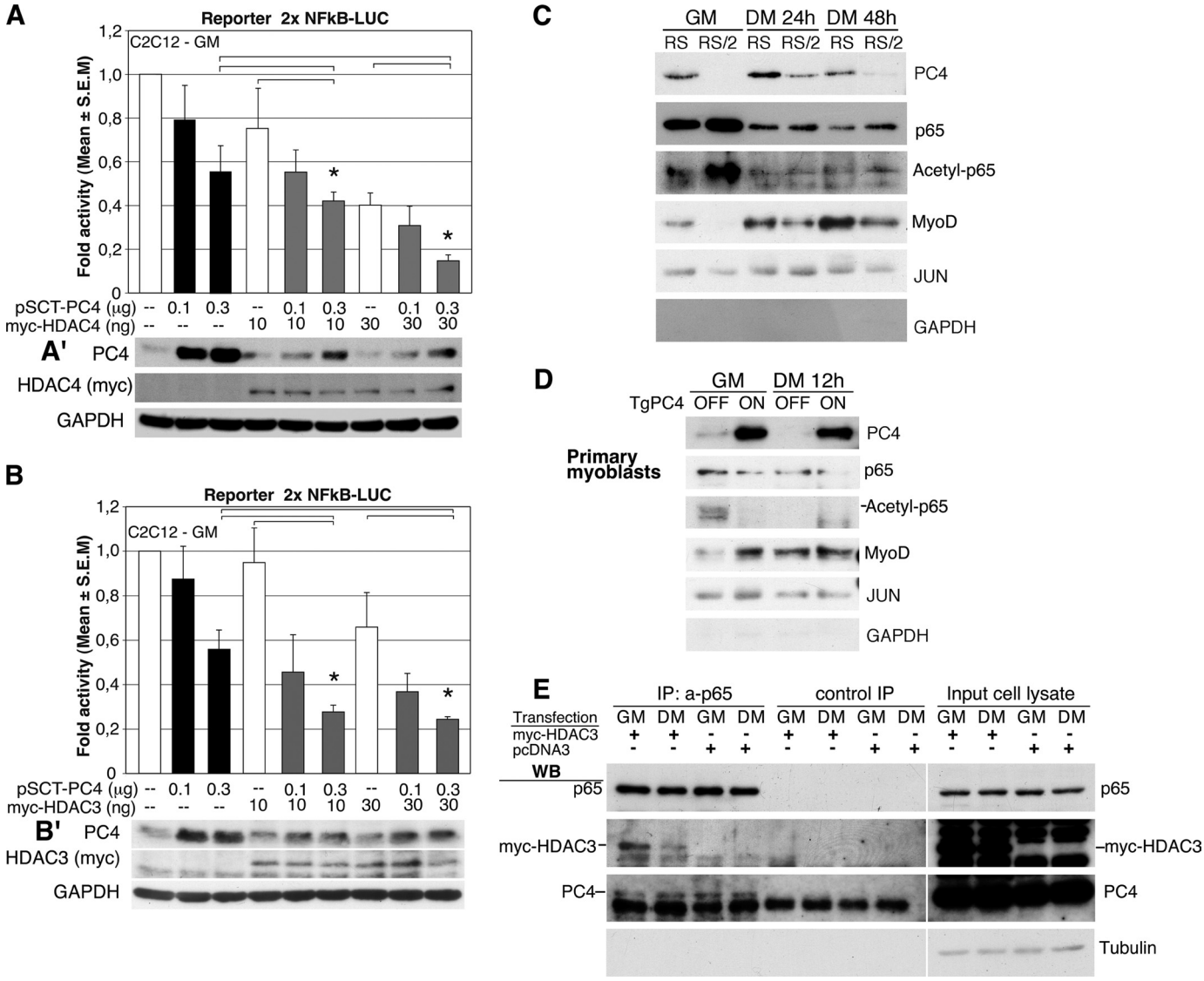

FIGURE 9. **PC4 represses the NF-κB transactivation function by promoting HDAC-dependent deacetylation of p65.** *A* and *B*, PC4 synergizes with HDAC4 or HDAC3 in inhibiting NF-κB activity. C2C12 cells, plated in duplicate 35-mm culture dishes (7×10^4 cells), were cotransfected the next day with the *NF-κB*-LUC reporter (0.1 μg), the pSCT-*PC4* (0.1–0.3 μg), and the pcDNA3-*myc-HDAC4* (10–30 ng) (*A*) or pcDNA3-myc-HDAC3 expression constructs (10–30 ng) (*B*). The pSCT and/or pcDNA3 empty vectors were included where necessary to normalize for DNA content. Cells were maintained in GM and harvested 48 h after transfection. Luciferase activity from cell extracts is calculated as fold change relative to the activity of the GM control sample transfected with the empty vectors. *Bars* represent the average fold activity ± S.E. determined from four independent experiments performed in duplicate. *, $p < 0.05$ *versus* the corresponding condition, as indicated (Student's *t* test). *A′* and *B′*, C2C12 cells transfected as in *A* and *B* were analyzed for PC4, myc-HDAC4, or myc-HDAC3 protein expression by Western blot. *C,* increased acetylation and nuclear localization of p65 in C2C12 cells deprived of *PC4*. Western blot analysis of nuclear extracts from C2C12 cells infected with the RS/2 retrovirus expressing shRNA to PC4 or the control retrovirus (*RS*), cultured in proliferating (GM) or differentiating conditions (DM 24 or 48 h). The same filter was probed with antibodies against PC4, p65, p65 acetylated at lysine 310 or MyoD, as well as c-Jun and GAPDH, markers of nuclear and cytoplasmic localization, respectively. *D,* decreased acetylation and nuclear localization of p65 in primary myoblasts isolated from adult muscle of the Tg *PC4* mouse. Nuclei were prepared from primary myoblasts derived from the Tg *PC4* mouse, cultured in proliferating (GM) or differentiating conditions (DM 12 h). *PC4* transgene was induced by administration of doxycycline to Tg *PC4* mice since conception and by addition of doxycycline to the medium (20 ng/ml) of primary myoblasts. The same filter was probed with antibodies against PC4, p65, p65 acetylated at lysine 310, MyoD, c-Jun or GAPDH. *E,* PC4 forms complexes with HDAC3 and p65. C2C12 cells (clone S4 constitutively overexpressing PC4) were transfected with pcDNA-*Myc-HDAC3* or the empty vector and cultured in GM or DM for 48 h as indicated. Cell lysates were immunoprecipitated with either anti-p65 antibody or control rabbit IgG, covalently bound to agarose beads. Immuno-complexes (*IP: a-p65* and *control IP*) and input cell lysates were analyzed by Western blotting (*WB*) with anti-Myc, anti-PC4 or anti-p65 antibodies. Input lysates: 1/15 of lysates used for immunoprecipitation.

blasts mediates the induction of *PC4* mRNA expression during the ensuing process of myogenic differentiation by stimulating the activity of the *PC4* gene promoter through a mechanism independent of MyoD binding to E-box motifs (13). We were now interested to define whether MyoD is nonetheless recruited to the *PC4* promoter. To this end we performed ChIP experiments in C2C12 myoblasts using an anti-MyoD antibody and amplifying a fragment of the mouse *PC4* gene (Tis7) promoter region. We observed that the MyoD protein was significantly recruited to the *PC4*/*Tis7* promoter, whereas the binding of MyoD to the *NeuroD1* negative control promoter was not above background levels (Fig. 10, *A* and *B*). This indicates that MyoD directly regulates *PC4* mRNA expression during differentiation. Notably, however, the MyoD protein was found to associate to the *PC4*/*Tis7* promoter not only during differentiation but also in prolifer-

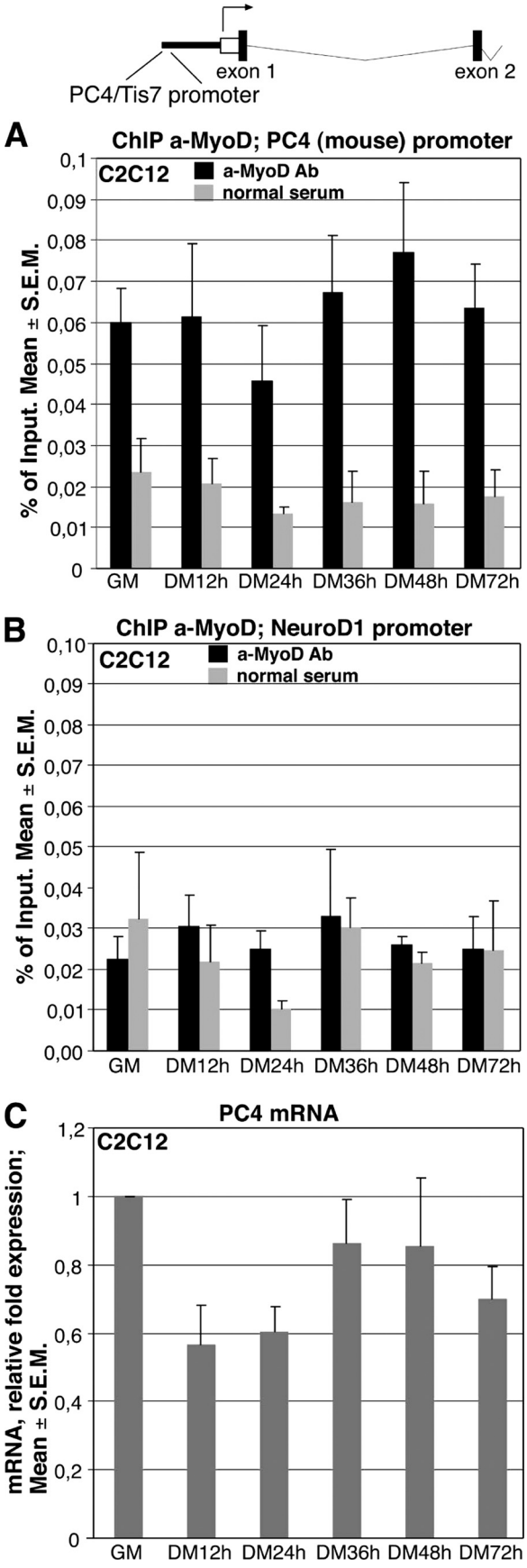

FIGURE 10. **MyoD is recruited to the *PC4* gene promoter.** *A,* ChIP analysis of MyoD binding to the mouse *PC4* promoter in proliferating (GM) or differentiating (DM) C2C12 myoblasts. The scheme *above* the graph illustrates the first exon of the mouse *PC4/Tis7* gene and the promoter region analyzed, located 780 nt before the transcription start. The amounts of *PC4* promoter region retrieved from immunoprecipitates obtained with anti-MyoD antibody (*black columns*) or with normal rabbit serum (*gray columns*) are expressed as percentage of the amounts of promoter region from input cell lysates. The same amount of chromatin was immunoprecipitated in ChIPs with a-MyoD or normal rabbit serum. *B,* ChIP analysis of MyoD binding to the *NeuroD1* promoter in C2C12 myoblasts, performed as negative control. *C, PC4* mRNA levels, detected by real time PCR in duplicate cultures of myoblasts analyzed by ChIP, expressed as fold values relative to the mRNA amount present in GM cultures. *A–C,* the average ± S.E. values are from three experiments.

ating myoblasts, *i.e.* in GM, where *MyoD* is transcriptionally inactive and *PC4* is expressed at levels similar to those of differentiating myoblasts (Fig. 10*C*). Indeed, as we have previously shown, *PC4* mRNA expression is positively regulated in proliferating conditions by serum growth factor-dependent mechanisms (13). The constitutive binding of MyoD to the *PC4* promoter suggests that *PC4* may belong to the category of genes directly activated by *MyoD* during differentiation through a feed-forward mechanism (58).

DISCUSSION

In this study, using gain and loss of function approaches, we show that *PC4* up-regulation in skeletal muscle *in vivo* stimulates regeneration and that the mechanism underlying this effect involves the control of MyoD by *PC4* through NF-κB.

In fact, in transgenic mice conditionally up-regulating *PC4* in adult skeletal muscle, we observed a significantly induced expression of *MyoD* and *myogenin* as well as that of several satellite cells markers, together with a remarkable increase of adult muscle regeneration following acute chemical damage. Conversely, the deprivation of *PC4* in adult satellite cell-derived C2C12 myoblasts produced the opposite effects, *i.e.* a dramatic impairment of myoblast fusion and greatly reduced expression of both *MyoD* and downstream differentiation markers, accompanied by an up-regulation of G_1-S cyclins, in particular cyclin D1. The induction of cyclin levels, detected in proliferating as well as differentiating conditions, led to a prolongation of the proliferative state of *PC4*-deprived myoblasts in differentiation medium. This effect was MyoD-dependent, because it was not observed in *PC4*-deprived C3H10T1/2 fibroblasts cultured in similar conditions, unless these cells were rendered myogenic through ectopic *MyoD* expression. This conclusion is consistent with the known ability of MyoD to inhibit cell cycle progression through several mechanisms, including induction of the retinoblastoma growth suppressor gene (*Rb*) and the cyclin-dependent kinase inhibitor *p21*, or its interaction with cyclin-dependent kinase 4 (CDK4) assembled to cyclin D1 (43, 44, 59–61). Furthermore, it is worth noting that proliferating $MyoD^{-/-}$ myoblasts cultured from knockout mice display increased levels of cyclins D and E that remain high after mitogen withdrawal (60), which is similar to what we observe in myoblasts expressing decreased MyoD levels as the consequence of *PC4* ablation.

Thus, the functional ablation of *PC4* in C2C12 differentiating myoblasts results in delayed exit from the cell cycle and impaired differentiation and fusion as the consequence of *MyoD* down-regulation. Furthermore, in this study we show that the down-regulation of MyoD by *PC4* relies on multiple mechanisms.

We have previously demonstrated that PC4 stimulates the transcriptional activity of MEF2C through displacement of HDAC4 from the MADS domain of MEF2C, because of its ability to bind both HDAC4 and MEF2C (13). MEF2 factors are known to participate in the autoregulatory loop exerted by MyoD on its own transcription (45, 46). Our present data indicate that the down-modulation of MyoD levels observed in the absence of *PC4* depends, at least in part, on a reduced activity of MEF2C.

Because, however, in the absence of *PC4* the most evident decrease of MyoD levels occurred in proliferating myoblasts, *i.e.* when MEF2C is not expressed (62), the deprivation of *PC4* also inhibited the levels of *MyoD* transcript produced from a transfected expression construct under the control of a heterologous promoter, and a further *PC4*-dependent mechanism controlling *MyoD* mRNA levels post-transcriptionally is conceivably operating in myoblasts. A key observation made in our study is that the deprivation of *PC4* or its overexpression in myoblasts significantly stimulates or inhibits, respectively, the transcriptional activity of NF-κB, revealing that *PC4* is a negative regulator of NF-κB. This is a noteworthy finding, because NF-κB is known to function as an inhibitor of skeletal myogenesis through several mechanisms (47, 54, 63, 64), including suppression of *MyoD* mRNA expression at the post-transcriptional level (47).

We show that *PC4* synergizes with HDAC4 and HDAC3 to inhibit the NF-κB transcriptional activity. It is known that the activity of NF-κB is critically controlled by acetylation. In particular, HDAC3, by deacetylating the p65 subunit of NF-κB, favors its binding to the IκBα repressor, with consequent nuclear export and relocalization into the cytoplasm of the p65-IκBα complex (52, 53, 55). Thus, we hypothesized that PC4 may facilitate the recruitment of HDAC3 to p65. Indeed, our immunoprecipitation experiments show that PC4 can form trimolecular complexes with HDAC3 and p65. Strong support for the idea that PC4 may favor the recruitment of HDACs to p65, thus promoting deacetylation and hence inactivation of p65, comes from the observations that primary myoblasts overexpressing transgenic *PC4* display reduced levels of acetylated p65, although deprivation of PC4 in myoblasts results in an increase of acetylated p65. In further agreement with the model proposed, we also find that overexpression of *PC4* causes a parallel decrease of nuclear p65, although the absence of *PC4* leads to accumulation of p65 in the nucleus, where p65 exerts its action. Notably, up-regulation of transgenic *PC4* in primary myoblasts induces MyoD levels in concomitance with deacetylation of p65 and a decrease of p65 levels in the nucleus, indicating that PC4 can control MyoD through p65 also *in vivo*.

In activated neutrophils, PC4 has been recently shown to associate with NF-κB p65 and HDAC1 (65). However, we identify here for the first time PC4 as a negative regulator of NF-κB activity, and in skeletal muscle this is relevant because the activation of NF-κB activity has been linked with disease states such as cachexia and various dystrophinopathies, although disruption of the NF-κB pathway inhibits skeletal muscle atrophy (66–68). In particular, a recent study has shown that in Duchenne muscular dystrophy mouse models (mdx) and patients, NF-κB signaling is persistently elevated in dystrophic muscles, and its down-regulation results in improved pathology and muscle function in mdx mice, thus implicating NF-κB as a potential therapeutic target for Duchenne muscular dystrophy (69). Thus, *PC4* may behave as a pivotal regulator of muscle differentiation and regeneration, in physiological and pathological condition, acting as an upstream regulator of MyoD levels by corepressing NF-κB activity through HDACs.

It is also noteworthy that in the absence of *PC4* Myf5 levels increase, consistently with the notion that inactivation of *MyoD* in mice leads to up-regulation of *Myf5* (70). This may only partially compensate for *MyoD* down-regulation; in fact, Myf5 appears to substitute for MyoD during embryogenesis but not during regeneration in adult muscle (14, 70).

We also provide evidence that *PC4* transcription is directly regulated by MyoD; in fact, although we have previously shown that MyoD can transactivate the *PC4* promoter, here we report that MyoD is recruited to the promoter region of the endogenous *PC4* gene (13). Altogether, these findings point to the existence of a positive regulatory loop between MyoD and *PC4*, where *PC4* links the MyoD activity to that of NF-κB and MEF2C, acting as repressor or enhancer, respectively. Given that in both cases PC4 acts through HDACs, it follows that, depending on the target to which is associated, PC4 can act as coactivator or corepressor.

Interestingly, the activation of Tg *PC4* since embryogenesis induced significant increases in the number of satellite cells (*i.e.* $Pax7^+$ cells) and myofibers in adult mice, suggesting that *PC4* is also relevant during early postnatal muscle growth. In fact, satellite cells are myogenic progenitors set apart during late fetal development to give rise to proliferating myoblasts for postnatal muscle growth, in addition to homeostasis and repair of adult skeletal muscle (36, 39). Our data also show that PC4 positively regulates the expression of *Pax7 in vivo*. It has been suggested that the expression of *Pax7* may favor the self-renewal of satellite cells (71, 72). However, because it has been shown that Pax7 acts genetically upstream of *MyoD* (71, 73, 74), it seems unlikely that the PC4-dependent increase of *Pax7* expression is mediated through *MyoD*; instead, one possibility is that up-regulation of *PC4* during embryonic and postnatal development, by enhancing the *MyoD*-dependent process of differentiation, may also trigger the activity and the renewal of the pool of satellite cells.

Considering the dramatic decrease in the number of myogenic cells occurring in muscle degenerative pathologies such as Duchenne dystrophy, our data highlighting the ability of *PC4* to potentiate the regenerative process suggest that *PC4* might be further investigated as a therapeutic target.

REFERENCES

1. Braun, T., Bober, E., Winter, B., Rosenthal, N., and Arnold, H. H. (1990) *EMBO J.* **9,** 821–831
2. Braun, T., Buschhausen-Denker, G., Bober, E., Tannich, E., and Arnold, H. H. (1989) *EMBO J.* **8,** 701–709
3. Davis, R. L., Weintraub, H., and Lassar, A. B. (1987) *Cell* **51,** 987–1000
4. Edmondson, D. G., and Olson, E. N. (1989) *Genes Dev.* **3,** 628–640
5. Miner, J. H., and Wold, B. (1990) *Proc. Natl. Acad. Sci. U.S.A.* **87,** 1089–1093

6. Rhodes, S. J., and Konieczny, S. F. (1989) *Genes Dev.* **3,** 2050–2061
7. Berkes, C. A., and Tapscott, S. J. (2005) *Semin. Cell Dev. Biol.* **16,** 585–595
8. Lassar, A. B., Davis, R. L., Wright, W. E., Kadesch, T., Murre, C., Voronova, A., Baltimore, D., and Weintraub, H. (1991) *Cell* **66,** 305–315
9. Naya, F. J., and Olson, E. (1999) *Curr. Opin. Cell Biol.* **11,** 683–688
10. Black, B. L., Molkentin, J. D., and Olson, E. N. (1998) *Mol. Cell. Biol.* **18,** 69–77
11. Guardavaccaro, D., Ciotti, M. T., Schäfer, B. W., Montagnoli, A., and Tirone, F. (1995) *Cell Growth Differ.* **6,** 159–169
12. Vadivelu, S. K., Kurzbauer, R., Dieplinger, B., Zweyer, M., Schafer, R., Wernig, A., Vietor, I., and Huber, L. A. (2004) *Mol. Cell. Biol.* **24,** 3514–3525
13. Micheli, L., Leonardi, L., Conti, F., Buanne, P., Canu, N., Caruso, M., and Tirone, F. (2005) *Mol. Cell. Biol.* **25,** 2242–2259
14. Megeney, L. A., Kablar, B., Garrett, K., Anderson, J. E., and Rudnicki, M. A. (1996) *Genes Dev.* **10,** 1173–1183
15. Buanne, P., Incerti, B., Guardavaccaro, D., Avvantaggiato, V., Simeone, A., and Tirone, F. (1998) *Genomics* **51,** 233–242
16. Tirone, F., and Shooter, E. M. (1989) *Proc. Natl. Acad. Sci. U.S.A.* **86,** 2088–2092
17. Gossen, M., and Bujard, H. (1992) *Proc. Natl. Acad. Sci. U.S.A.* **89,** 5547–5551
18. Wiekowski, M. T., Chen, S. C., Zalamea, P., Wilburn, B. P., Kinsley, D. J., Sharif, W. W., Jensen, K. K., Hedrick, J. A., Manfra, D., and Lira, S. A. (2001) *J. Immunol.* **167,** 7102–7110
19. Hogan, B., Costantini, F., and Lacy, E. (1995) *Manipulating the Mouse Embryo: A Laboratory Manual,* 2nd Ed, Cold Spring Harbor Laboratory Press, Cold Spring Harbor, NY
20. Rando, T. A., and Blau, H. M. (1994) *J. Cell Biol.* **125,** 1275–1287
21. Brummelkamp, T. R., Bernards, R., and Agami, R. (2002) *Science* **296,** 550–553
22. Molkentin, J. D., Black, B. L., Martin, J. F., and Olson, E. N. (1996) *Mol. Cell. Biol.* **16,** 2627–2636
23. Lu, J., McKinsey, T. A., Zhang, C. L., and Olson, E. N. (2000) *Mol. Cell* **6,** 233–244
24. Fimia, G. M., Gottifredi, V., Bellei, B., Ricciardi, M. R., Tafuri, A., Amati, P., and Maione, R. (1998) *Mol. Biol. Cell* **9,** 1449–1463
25. Guenther, M. G., Barak, O., and Lazar, M. A. (2001) *Mol. Cell. Biol.* **21,** 6091–6101
26. Soddu, S., Blandino, G., Scardigli, R., Coen, S., Marchetti, A., Rizzo, M. G., Bossi, G., Cimino, L., Crescenzi, M., and Sacchi, A. (1996) *J. Cell Biol.* **134,** 193–204
27. Jacquemin, V., Butler-Browne, G. S., Furling, D., and Mouly, V. (2007) *J. Cell Sci.* **120,** 670–681
28. Guardavaccaro, D., Corrente, G., Covone, F., Micheli, L., D'Agnano, I., Starace, G., Caruso, M., and Tirone, F. (2000) *Mol. Cell. Biol.* **20,** 1797–1815
29. Chomczynski, P., and Sacchi, N. (1987) *Anal. Biochem.* **162,** 156–159
30. Livak, K. J., and Schmittgen, T. D. (2001) *Methods* **25,** 402–408
31. Farioli-Vecchioli, S., Tanori, M., Micheli, L., Mancuso, M., Leonardi, L., Saran, A., Ciotti, M. T., Ferretti, E., Gulino, A., Pazzaglia, S., and Tirone, F. (2007) *FASEB J.* **21,** 2215–2225
32. Heard, E., Rougeulle, C., Arnaud, D., Avner, P., Allis, C. D., and Spector, D. L. (2001) *Cell* **107,** 727–738
33. Buskin, J. N., and Hauschka, S. D. (1989) *Mol. Cell. Biol.* **9,** 2627–2640
34. Baeza-Raja, B., and Muñoz-Cánoves, P. (2004) *Mol. Biol. Cell* **15,** 2013–2026
35. Kistner, A., Gossen, M., Zimmermann, F., Jerecic, J., Ullmer, C., Lübbert, H., and Bujard, H. (1996) *Proc. Natl. Acad. Sci. U.S.A.* **93,** 10933–10938
36. Chargé, S. B., and Rudnicki, M. A. (2004) *Physiol. Rev.* **84,** 209–238
37. Yablonka-Reuveni, Z., Day, K., Vine, A., and Shefer, G. (2008) *J. Anim. Sci.* **86,** E207–E216
38. Sartorelli, V., and Fulco, M. (2004) *Sci. STKE 2004,* re11
39. Sabourin, L. A., and Rudnicki, M. A. (2000) *Clin. Genet.* **57,** 16–25
40. Blau, H. M., Chiu, C. P., and Webster, C. (1983) *Cell* **32,** 1171–1180
41. Weinberg, R. A. (1995) *Cell* **81,** 323–330
42. Welcker, M., and Clurman, B. (2005) *Curr. Biol.* **15,** R810–R812
43. Crescenzi, M., Fleming, T. P., Lassar, A. B., Weintraub, H., and Aaronson, S. A. (1990) *Proc. Natl. Acad. Sci. U.S.A.* **87,** 8442–8446
44. Sorrentino, V., Pepperkok, R., Davis, R. L., Ansorge, W., and Philipson, L. (1990) *Nature* **345,** 813–815
45. Thayer, M. J., Tapscott, S. J., Davis, R. L., Wright, W. E., Lassar, A. B., and Weintraub, H. (1989) *Cell* **58,** 241–248
46. L'honore, A., Rana, V., Arsic, N., Franckhauser, C., Lamb, N. J., and Fernandez, A. (2007) *Mol. Biol. Cell* **18,** 1992–2001
47. Guttridge, D. C., Mayo, M. W., Madrid, L. V., Wang, C. Y., and Baldwin, A. S., Jr. (2000) *Science* **289,** 2363–2366
48. Rossi, A., Kapahi, P., Natoli, G., Takahashi, T., Chen, Y., Karin, M., and Santoro, M. G. (2000) *Nature* **403,** 103–108
49. Hayden, M. S., and Ghosh, S. (2008) *Cell* **132,** 344–362
50. Traenckner, E. B., Pahl, H. L., Henkel, T., Schmidt, K. N., Wilk, S., and Baeuerle, P. A. (1995) *EMBO J.* **14,** 2876–2883
51. Karin, M., and Ben-Neriah, Y. (2000) *Annu. Rev. Immunol.* **18,** 621–663
52. Ashburner, B. P., Westerheide, S. D., and Baldwin, A. S., Jr. (2001) *Mol. Cell. Biol.* **21,** 7065–7077
53. Chen, L. F., Mu, Y., and Greene, W. C. (2002) *EMBO J.* **21,** 6539–6548
54. Bakkar, N., Wang, J., Ladner, K. J., Wang, H., Dahlman, J. M., Carathers, M., Acharyya, S., Rudnicki, M. A., Hollenbach, A. D., and Guttridge, D. C. (2008) *J. Cell Biol.* **180,** 787–802
55. Chen, Lf, Fischle, W., Verdin, E., and Greene, W. C. (2001) *Science* **293,** 1653–1657
56. Vietor, I., Vadivelu, S. K., Wick, N., Hoffman, R., Cotten, M., Seiser, C., Fialka, I., Wunderlich, W., Haase, A., Korinkova, G., Brosch, G., and Huber, L. A. (2002) *EMBO J.* **21,** 4621–4631
57. Chen, L. F., and Greene, W. C. (2003) *J. Mol. Med.* **81,** 549–557
58. Tapscott, S. J. (2005) *Development* **132,** 2685–2695
59. Martelli, F., Cenciarelli, C., Santarelli, G., Polikar, B., Felsani, A., and Caruso, M. (1994) *Oncogene* **9,** 3579–3590
60. Kitzmann, M., and Fernandez, A. (2001) *Cell. Mol. Life Sci.* **58,** 571–579
61. Zhang, J. M., Zhao, X., Wei, Q., and Paterson, B. M. (1999) *EMBO J.* **18,** 6983–6993
62. McDermott, J. C., Cardoso, M. C., Yu, Y. T., Andres, V., Leifer, D., Krainc, D., Lipton, S. A., and Nadal-Ginard, B. (1993) *Mol. Cell. Biol.* **13,** 2564–2577
63. Guttridge, D. C., Albanese, C., Reuther, J. Y., Pestell, R. G., and Baldwin, A. S., Jr. (1999) *Mol. Cell. Biol.* **19,** 5785–5799
64. Wang, H., Hertlein, E., Bakkar, N., Sun, H., Acharyya, S., Wang, J., Carathers, M., Davuluri, R., and Guttridge, D. C. (2007) *Mol. Cell. Biol.* **27,** 4374–4387
65. Gu, Y., Harley, I. T., Henderson, L. B., Aronow, B. J., Vietor, I., Huber, L. A., Harley, J. B., Kilpatrick, J. R., Langefeld, C. D., Williams, A. H., Jegga, A. G., Chen, J., Wills-Karp, M., Arshad, S. H., Ewart, S. L., Thio, C. L., Flick, L. M., Filippi, M. D., Grimes, H. L., Drumm, M. L., Cutting, G. R., Knowles, M. R., and Karp, C. L. (2009) *Nature* **458,** 1039–1042
66. Monici, M. C., Aguennouz, M., Mazzeo, A., Messina, C., and Vita, G. (2003) *Neurology* **60,** 993–997
67. Hunter, R. B., and Kandarian, S. C. (2004) *J. Clin. Invest.* **114,** 1504–1511
68. Baghdiguian, S., Martin, M., Richard, I., Pons, F., Astier, C., Bourg, N., Hay, R. T., Chemaly, R., Halaby, G., Loiselet, J., Anderson, L. V., Lopez de Munain, A., Fardeau, M., Mangeat, P., Beckmann, J. S., and Lefranc, G. (1999) *Nat. Med.* **5,** 503–511
69. Acharyya, S., Villalta, S. A., Bakkar, N., Bupha-Intr, T., Janssen, P. M., Carathers, M., Li, Z. W., Beg, A. A., Ghosh, S., Sahenk, Z., Weinstein, M., Gardner, K. L., Rafael-Fortney, J. A., Karin, M., Tidball, J. G., Baldwin, A. S., and Guttridge, D. C. (2007) *J. Clin. Invest.* **117,** 889–901
70. Rudnicki, M. A., Braun, T., Hinuma, S., and Jaenisch, R. (1992) *Cell* **71,** 383–390
71. Zammit, P. S., Relaix, F., Nagata, Y., Ruiz, A. P., Collins, C. A., Partridge, T. A., and Beauchamp, J. R. (2006) *J. Cell Sci.* **119,** 1824–1832
72. Oustanina, S., Hause, G., and Braun, T. (2004) *EMBO J.* **23,** 3430–3439
73. Seale, P., Ishibashi, J., Holterman, C., and Rudnicki, M. A. (2004) *Dev. Biol.* **275,** 287–300
74. Relaix, F., Rocancourt, D., Mansouri, A., and Buckingham, M. (2005) *Nature* **435,** 948–953